ON MODEL ATMOSPHERES FOR THE HIGH-TEMPERATURE STARS

BY

ANNE B. UNDERHILL

1. The temperatures of the early-type stars are not known very precisely inspite of a number of investigations to establish the upper end of the temperature scale. This state of affairs is a result partly of the complex and largely unknown relationships existing between the various types of temperature which may be defined, and partly of the observational difficulties. The methods of colour temperature are inconclusive for the high temperature stars because in the O and B stars most of the flux is emitted at inaccessible wavelengths in the far ultraviolet, hence measurements can only be made on the tail of the energy distribution curve where the gradient is not very sensitive to temperature, and because the spectral distribution of the photographic and visual light received from most O and B stars is modified by the interstellar material lying between these stars and us. The ionisation temperature scale introduced by Fowler and Milne (1) and used extensively by Miss Payne (2) and also by Pannekoek (3), has been the most useful temperature scale for the early-type stars, but for the earliest types it is somewhat uncertain as it depends entirely upon the spectral type chosen typical of the He^{++} maximum. R. M. Petrie (4) has discussed critically the existing temperature scales for the early type stars and in particular criticises Kuiper's (5) extrapolated ionisation temperature scale. Petrie has proposed a more compressed excitation temperature scale, but because his results are based on a single curve of growth for $He\ I$ which is used for all the stars and because of the sensitivity to Stark effect of the lines of $He\ I$ and $He\ II$ which he uses, it is doubtful if the method he has used is very sensitive. In any case it is not clear that ionisation temperature, excitation temperature and effective

1*

temperature should be closely the same for the early type stars. UNSÖLD's (6) investigations of the atmosphere of τSco, a $BO\ V$ star, show the difficulties to be met in trying to establish from observations an exact ionisation or excitation temperature for the early-type stars, and clearly point to the intricate relationship existing in a stellar atmosphere between the various temperatures which may be defined.

In view of the differing observational results that have been obtained, a theoretical determination of the effective temperature of an early-type atmosphere would be valuable. The method of model atmospheres offers a powerful tool for determining effective temperature, for, once an acceptable model atmosphere has been obtained, the integrated net flux emerging from it may be calculated. By definition the integrated net flux determines the effective temperature of the atmosphere. This temperature will be the effective temperature of the spectral type corresponding to the model atmosphere. In this paper, methods for computing model atmospheres for the high temperature stars and for determining the spectra of these atmospheres will be developed and a model atmosphere will be computed. The spectral type of this model atmosphere will be determined by comparison with observations and the emergent flux will be calculated in detail so that the effective temperature of the model atmosphere may be found and a point determined at the upper end of the stellar temperature scale.

Recently the method of model atmospheres has been highly developed by STRÖMGREN (7) and applied by Strömgren and his co-workers to studies of the solar atmosphere and of the atmospheres of stars of neighbouring spectral type, while RUD-KJØBING (8) has applied these ideas to the study of the atmospheres of B-type stars. We shall proceed in a manner somewhat different in detail from that adopted by Rudkjøbing, who uses the principle of the Rosseland mean absorption coefficient and divides the radiation field into two parts and then works with only the flux at frequencies greater than the Lyman limit to get the structure of his atmosphere, for we shall work with the whole radiation field and we shall use the CHANDRASEKHAR straight mean absorption coefficient (9) which is particularly advantageous for dealing with the effects of radiation pressure on the

mechanical equilibrium of the atmosphere (10). With a view to
the extension of the method of model atmospheres to atmospheres
of very high effective temperature, we shall consider the effects
of radiation pressure in more detail than has been the case in
previous investigations. Like Rudkjøbing we shall assume that
the opacity in our model atmosphere is given by continuous
absorption from hydrogen and helium, which are present in the
ratio 85:15 by number, and by electron scattering. We shall go
further than Rudkjøbing in that we shall test our model atmo-
sphere for radiative equilibrium by computing the net flux without
making any approximations at all. We shall also discuss in detail
the question of the f-values for the lines of L-S coupling multiplets,
and will assemble the necessary formulae for computing these
f-values. The method, due to Strömgren, which we will use for
computing the net flux in the atmosphere by solving the Schwarz-
schild integral equation, provides us with a non-approximate
method of calculating the line spectrum of the model atmosphere.
A by-product of these calculations is the limb-darkening of the
model atmosphere in various wave-lengths.

Numerical methods, such as we will use, give a realistic
picture of the stellar atmosphere, for they take account of the
actual variation of the quantities in the atmosphere, and make
no a priori assumptions about the behaviour of any of these
quantities. The model atmosphere is idealised to the extent that
it is assumed to be symmetrical with respect to the centre of the
star so that the physical parameters vary with depth in the
atmosphere only, and it is assumed that the chemical com-
position is constant throughout the atmosphere. Furthermore the
atmosphere is assumed to be in a state of mechanical equilibrium.
The dependence of temperature upon the pressure and the
electron pressure throughout the atmosphere is then obtained by
integrating the differential equation of mechanical equilibrium.
The model atmosphere so obtained is said to represent a real
stellar atmosphere in radiative equilibrium if it can be shown
that an atmosphere with this structure produces a net flux which
is constant with increasing optical depth. When a model atmo-
sphere satisfying the two conditions of mechanical equilibrium
and constant net flux has been obtained, the line spectrum of
the model atmosphere may be calculated and detailed information

about the spectral type of the model atmosphere and the abund-
ance of the elements in the stars may be derived by comparing
the computed spectrum with observed spectra.

2. We shall consider an atmosphere of high effective temper-
ature in which the opacity is a result of continuous absorption
by hydrogen, neutral helium and ionised helium, and of electron
scattering. We shall further assume that the star is a main-
sequence star and that the transport of energy by turbulence is
not important. The equation for mechanical equilibrium in such
an atmosphere is

$$\frac{d\,(p_g + p_r)}{dz} = -g\varrho \tag{1}$$

where p_g is the gas pressure, p_r is the radiation pressure, and ϱ
is the density at the level z in the atmosphere. The surface gravity
of the star is g. In atmospheres of comparatively low effective
temperature the radiation pressure is negligible in comparison to
the gas pressure. However, in atmospheres of high effective
temperature the radiation pressure is not negligible. In an atmo-
sphere in which the opacity is given by continuous absorption
and by electron scattering it may be shown (10) that

$$\frac{dp_r}{dz} = -\frac{\pi}{c}\int_0^\infty (\varkappa_\nu + \sigma)\,\varrho\,F_\nu\,d\nu, \tag{2}$$

where $\varkappa_\nu$ is the monochromatic mass-absorption coefficient in
the atmoshpere and σ is the mass-scattering coefficient assumed
to be independent of wavelength. In such an atmosphere (11)
the gray-body temperature law deduced by CHANDRASEKHAR (9)
remains a valid approximation if the optical depth is defined by

$$d\tau = -(\bar{\varkappa} + \sigma)\,\varrho\,dz \tag{3}$$

where

$$\varkappa_\nu = \bar{\varkappa}\,(1 + \delta_\nu), \tag{4}$$

and if $\bar{\varkappa}$ is defined formally in the manner recommended by
CHANDRASEKHAR (9), that is if

$$\bar{\varkappa} = \int_0^\infty \varkappa_\nu\,\frac{F_\nu^{(1)}}{F}\,d\nu. \tag{5}$$

Here $F_\nu^{(1)}$ is the monochromatic flux in a gray atmosphere in which the opacity is given by continuous absorption and by continuous scattering. In CHANDRASEKHAR's discussion the opacity in the atmosphere is given by absorption only. The quantity δ_ν is a small quantity giving the departure from grayness at any frequency. When we introduce equation (4) into equation (2) we find

$$\frac{dp_r}{dz} = -\frac{\pi}{c}(\bar{\varkappa}+\sigma)\varrho\int_0^\infty F_\nu\, d\nu - \frac{\pi}{c}\bar{\varkappa}\varrho\int_0^\infty \delta_\nu F_\nu\, d\nu. \qquad (6)$$

We can be reasonably sure that the second term on the right side of equation (6) is small since the definition of $\bar{\varkappa}$ (eq. [5]) is equivalent to putting

$$\int_0^\infty \delta_\nu F_\nu^{(1)}\, d\nu = 0,$$

and we may expect that the actual monochromatic flux F_ν, is of the same order of magnitude as the gray-body monochromatic flux, $F_\nu^{(1)}$. We shall neglect the second term and write

$$\frac{dp_r}{dz} = -\frac{\pi}{c}(\bar{\varkappa}+\sigma)\varrho\int_0^\infty F_\nu\, d\nu, \qquad (7)$$

that is we shall use the radiation pressure gradient of a gray-atmosphere. The definition of effective temperature gives

$$\pi\int_0^\infty F_\nu\, d\nu = \sigma_R T_e^4 \qquad (8)$$

where σ_R is the radiation constant, $5\cdot67\times10^{-5}$ ergs/cm²/sec/degree⁴. Hence we have

$$\frac{dp_r}{dz} = -(\bar{\varkappa}+\sigma)\varrho\frac{\sigma_R}{c}T_e^4. \qquad (9)$$

If we introduce this expression into equation (1) and change to the variable τ, optical depth, we find that the equation for mechanical equilibrium including the effect of radiation pressure is

$$\frac{dp_g}{d\tau} = \frac{g}{\bar{\varkappa}+\sigma} - \frac{\sigma_R}{c}T_e^4. \qquad (10)$$

We shall determine the structure of our atmosphere by integrating this equation. The term $(\sigma_R/c)\, T_e^4$ is a constant for any atmosphere. In atmospheres of low effective temperature this term, representing the effect of radiation pressure, is negligible. However, when T_e is greater than 10^4 this term becomes important. This treatment, which is possible only if a straight mean absorption coefficient is used, becomes more accurate as the departures from grayness, δ_ν, become small, and the value of the neglected term approaches zero. This method has the advantage that we use the true surface gravity of the star in integrating our atmosphere rather than an effective surface gravity which is not necessarily constant with depth. That g_{eff} is not necessarily constant with depth may be seen from its usual definition, (12)

$$g_{\text{eff}} = g + \frac{1}{\varrho}\frac{dp_r}{dz}. \tag{11}$$

We have no a priori reason for supposing the term $\varrho^{-1}\, dp_r/dz$ to be constant with depth, and indeed reference to equation (6) will show in general that this term is not constant with depth for $\bar{\varkappa} + \sigma$ and $\bar{\varkappa}$ are not constant with depth. In cases where g_{eff} is very nearly the same as g, the possible variations in g_{eff} are of little account.

In order to integrate equation (10) and obtain the structure of the atmosphere we must know the dependence of $\bar{\varkappa} + \sigma$ on τ. (We shall use the parameter τ as the independent variable in the integration). First we need to know the relation between τ and T, the temperature at any level in the atmosphere, for $\bar{\varkappa}$ depends on T. Analytical studies, (9), (11), have given relations between τ and T which are valid in a gray atmosphere and which should be good approximations in a non-gray atmosphere. However, on integrating a model atmosphere it is immaterial exactly what $\tau - T$ relation we use so long as we obtain an atmosphere which is in mechanical equilibrium and which yields a constant net flux. As a first approximation we shall use the classical relation

$$T(\tau)^4 = T_0^4\left(1 + \frac{3}{2}\tau\right), \tag{12}$$

where T_0 is the boundary temperature. If the flux from our model is not constant with depth we shall modify this relation in a second approximation.

The opacity of our atmosphere is given by hydrogen, helium and by electron scattering. We assume hydrogen and helium to be present in the proportion 85:15 by number. We can neglect the small amounts of the other elements present, for these elements do not contribute appreciably to the opacity of the atmosphere. The mixture chosen is such that one gram of star material contains 0.585 grams of hydrogen and 0.415 grams of helium. If $k_\nu (H)$ is the monochromatic continuous absorption coefficient of hydrogen per gram of neutral hydrogen, $k_\nu (He\, I)$ is the monochromatic continuous absorption coefficient of neutral helium per gram of neutral helium, and $k_\nu (He\, II)$ is the monochromatic continuous absorption coefficient of ionised helium per gram of once-ionised helium, then the monochromatic continuous absorption coefficient per gram of star material is

$$\varkappa_\nu = 0 \cdot 585 \, (1 - x_H) \, k_\nu \, (H) + 0 \cdot 415 \, (1 - x_{He\,I} - x_{He\,II}) \, k_\nu \, (He\,I)$$

$$+ \, 0 \cdot 415 \, x_{He\,I} \, k_\nu \, (He\,II). \tag{13}$$

Here x_H is the degree of ionisation of hydrogen, $x_{He\,I}$ gives the fraction of singly ionised helium atoms, and $x_{He\,II}$ gives the fraction of doubly ionised helium atoms. The absorption coefficients $k_\nu \, (H)$, $k_\nu \, (He\, I)$, $k_\nu \, (He\, II)$ depend only on the temperature, or optical depth, whereas the abundance factors, $0 \cdot 585$ $(1 - x_H)$, etc., depend on the temperature and the electron pressure. These factors may be calculated from the ionisation equation. We have

$$\log \frac{x_H}{1 - x_H} = - \, 13 \cdot 53 \, \theta + \frac{5}{2} \log T - 0 \cdot 477 - \log p_e, \tag{14}$$

$$\log \frac{N_{He^+}}{N_{He^0}} = \log A = - \, 24 \cdot 46 \, \theta + \frac{5}{2} \log T + 0 \cdot 125 - \log p_e, \tag{15}$$

and

$$\log \frac{N_{He^{++}}}{N_{He^+}} = \log B = - \, 54 \cdot 14 \, \theta + \frac{5}{2} \log T - 0 \cdot 477 - \log p_e, \tag{16}$$

where we have put $\theta = 5040/T$. Since we define

$$x_{He\,I} = N_{He^+}/N_{He}$$

and

$$x_{He\,II} = N_{He^{++}}/N_{He}$$

where N_{He} is the total number of helium atoms and ions present, it follows that

$$x_{He\,I} = \frac{A}{1 + A\,(1 + B)} = \frac{1}{1 + B} \tag{17}$$

and

$$x_{He\,II} = \frac{AB}{1 + A\,(1 + B)} = \frac{B}{(1 + B)}. \tag{18}$$

The quantities A and B are found from equations (15) and (16). From equations (5) and (13) it follows that

$$\bar{z} = 0 \cdot 585\,(1 - x_H)\,\bar{k}\,(H) + 0 \cdot 415\,(1 - x_{He\,I} - x_{He\,II})\,\bar{k}\,(He\,I)$$
$$+ 0 \cdot 415\,x_{He\,I}\,\bar{k}\,(He\,II), \tag{19}$$

where

$$\left.\begin{array}{l}
\bar{k}\,(H) = \displaystyle\int_0^\infty k_\nu\,(H)\,\frac{F_\nu^{(1)}}{F}\,d\nu, \\[4mm]
\bar{k}\,(He\,I) = \displaystyle\int_0^\infty k_\nu\,(He\,I)\,\frac{F_\nu^{(1)}}{F}\,d\nu, \\[4mm]
\bar{k}\,(He\,II) = \displaystyle\int_0^\infty k_\nu\,(He\,II)\,\frac{F_\nu^{(1)}}{F}\,d\nu.
\end{array}\right\} \tag{20}$$

The coefficient of scattering per gram of star material is $\sigma = \sigma_e \times$ number of electrons per gram of star material where σ_e is the scattering coefficient per electron, $8\,\pi e^4/3\,m^2 c^4$. We find that

$$\sigma = \sigma_e \left[\frac{0 \cdot 585}{m_H}\,x_H + \frac{0 \cdot 415}{m_{He}}\,(x_{He\,I} + 2\,x_{He\,II})\right],$$

where m_H is the mass of the hydrogen atom and $m_{He} = 4\,m_H$ is the mass of the helium atom. When the numerical factors are introduced we obtain

$$\sigma = 0 \cdot 397\,\left[0 \cdot 585\,x_H + 0 \cdot 104\,(x_{He\,I} + 2\,x_{He\,II})\right]. \tag{21}$$

The coefficient of scattering per gram of star material depends on the electron pressure and the temperature at any level in the atmosphere. The maximum value σ can reach, ($x_H = 1, x_{He\,I} = 0$, $x_{He\,II} = 1$), is 0·315 with the mixture of H and He used.

The monochromatic absorption coefficients for hydrogen and for ionised helium corrected for stimulated emission can readily be found from Kramers law. The development of these formula is discussed for instance by UNSÖLD [(12), p. 117 ff.]. We have

$$k_\nu(H) = \frac{F(H)\,D(H)}{u^3}(1 - e^{-u}),\qquad(22)$$

where

$$F(H) = \frac{64\,\pi^4\;me^{10}\;e^{-u_1(H)}}{3\sqrt{3}\;ch^3\,m_H\,(kT)^3}$$

and

$$D(H) = \sum_{\substack{1 < n}}^{n=9}\frac{e^{u_n(H)}}{n^3} + \frac{e^{u_{10}(H)}}{2_{u_1}(H)}.$$

Here we have extended Unsöld's treatment by continuing the summation over all continua up to that from the level $n = 9$, and then have performed an integration. The abreviation $u = h\nu/kT$ is used. The quantity $u_n(H)$ is the value of u at the series limit n,

$$u_n(H) = \frac{1}{n^2}\frac{R_H\,hc}{kT}$$

where R_H is the Rydberg constant for hydrogen. Values of $F(H)D(H)$ for hydrogen at a number of temperatures are given in Table 1. From this information $k_\nu(H)$ may be readily calculated by equation (22) for any temperature and at any wavelength desired.

Since the ionised helium atom is hydrogen-like, we may find the continuous absorption coefficient of ionised helium corrected for stimulated emission in the same way. We have

$$k_\nu(He\,II) = \frac{F(He\,II)\,D(He\,II)}{u^3}(1 - e^{-u}),\qquad(23)$$

where

$$F(HeII) = \frac{64\,\pi^4}{3\sqrt{3}}\;\frac{me^{10}}{ch^3\,m_{He}}\;\frac{(2^4)\,e^{-u_1\,(He\,I)}}{(kT)^3}$$

and

$$D(H) = \sum_{1<n}^{n=9} \frac{e^{u_n\,(He\,II)}}{n^3} + \frac{e^{u_{10}\,(He\,II)}}{2\,u^1\,(He\,II)}.$$

The quantity $u_n\,(He\,II)$ is

$$u_n\,(He\,II) = \frac{4}{n^2}\,R_{He}\,\frac{hc}{kT}$$

where R_{He} is the Rydberg constant for helium. Values of $F\,(He\,II)$ $D\,(He\,II)$ at a number of temperatures are given in Table 2.

Table 1.

$F(H) \cdot D(H)$ per gram of neutral hydrogen.

T	$0 < \lambda < 911.6\,\mathrm{A}^*$	$911.6 < \lambda < 3646\,\mathrm{A}^*$	$3646 < \lambda < 8204\,\mathrm{A}^*$	$8204 < \lambda < 14{,}590\,\mathrm{A}^*$
$25{,}200°$	1.17×10^9	1.81×10^6	4.65×10^5	2.99×10^5
$28{,}000$	8.49×10^8	2.16	6.20×10^5	4.12×10^5
$30{,}000$	6.96×10^8	2.37	7.50×10^5	5.14×10^5
$32{,}000$	5.73×10^8	2.62	8.69×10^5	6.08×10^5
$34{,}000$	4.80×10^8	2.81	9.90×10^5	7.07×10^5
$38{,}000$	3.42×10^8	3.06	1.19×10^6	8.74×10^5
$42{,}000$	2.54×10^8	3.22	1.36×10^6	1.04×10^6
$46{,}000$	1.96×10^8	3.48	1.61×10^6	1.27×10^6
$50{,}000$	1.52×10^8	3.34	1.64×10^6	1.33×10^6
$54{,}000$	1.22×10^8	3.42	1.69×10^6	1.37×10^6
$58{,}000$	9.90×10^7	3.28	1.73×10^6	1.43×10^6
$62{,}000$	8.15×10^7	3.21	1.76×10^6	1.46×10^6
$70{,}000$	5.74×10^7	3.08	1.81×10^6	1.54×10^6
$80{,}000°$	3.92×10^7	2.76×10^6	1.73×10^6	1.49×10^6

* vacuum wavelengths.

We neglect the Gaunt factors in calculating k_ν, for reference to a review of the question of the values of the Gaunt factors by CHANDRASEKHAR (13) shows that the Gaunt factors are close to unity except near the series limit and in the region $\nu \to \infty$. In the latter region $g\,(\nu,\,n) \to 0$, but this fact is of little importance for the contribution of $\bar{k}_\nu$ to $\bar{k}$ at the very highest frequencies is

Table 2.

$F(He\ II)\cdot D(He\ II)$ per gram of ionised helium.

T	$0<\lambda<228\,\mathrm{A}$	$228<\lambda<912\,\mathrm{A}$	$912<\lambda<2052\,\mathrm{A}$	$2052<\lambda<3646\,\mathrm{A}$
25,200°	4.74×10^{9}	4.05	4.47×10^{-2}	8.57×10^{-3}
28,000	3.40×10^{9}	19.2	0.312	6.93×10^{-2}
30,000	2.76×10^{9}	48.7	1.18	2.41×10^{-1}
32,000	2.28×10^{9}	1.08×10^{2}	2.70	7.15×10^{-1}
34,000	1.90×10^{9}	2.17×10^{2}	6.54	1.86
38,000	1.36×10^{9}	6.75×10^{2}	27.9	8.95
42,000	9.95×10^{8}	1.65×10^{3}	88.2	31.4
46,000	7.68×10^{8}	3.46×10^{3}	2.29×10^{2}	88.8
50,000	6.93×10^{8}	7.64×10^{3}	6.22×10^{2}	2.60×10^{2}
54,000	4.73×10^{8}	1.01×10^{4}	9.50×10^{2}	4.18×10^{2}
58,000	3.05×10^{8}	1.21×10^{4}	1.31×10^{3}	6.09×10^{2}
62,000	3.14×10^{8}	2.13×10^{4}	2.62×10^{3}	1.28×10^{3}
70,000	2.18×10^{8}	3.67×10^{4}	5.59×10^{3}	2.95×10^{3}
80,000°	1.45×10^{8}	1.03×10^{5}	5.43×10^{4}	6.40×10^{3}

T	$3646<\lambda<5698\,\mathrm{A}$	$5698<\lambda<8204\,\mathrm{A}$	$8204<\lambda<11{,}170\,\mathrm{A}$	$11{,}170<\lambda<14{,}590\,\mathrm{A}$
25,200°	4.02×10^{-3}	2.70×10^{-3}	2.14×10^{-3}	1.85×10^{-3}
28,000	3.51×10^{-2}	2.45×10^{-2}	1.98×10^{-2}	1.74×10^{-2}
30,000	1.27×10^{-1}	9.11×10^{-2}	7.49×10^{-2}	6.61×10^{-2}
32,000	3.93×10^{-1}	2.87×10^{-1}	2.39×10^{-1}	2.13×10^{-1}
34,000	1.05	7.84×10^{-1}	6.59×10^{-1}	5.90×10^{-1}
38,000	5.39	4.13	3.54	3.21
42,000	19.8	15.6	13.5	12.4
46,000	58.3	46.8	41.1	37.8
50,000	1.77×10^{2}	1.45×10^{2}	1.29×10^{2}	1.19×10^{2}
54,000	2.93×10^{2}	2.42×10^{2}	2.19×10^{2}	2.03×10^{2}
58,000	4.34×10^{2}	3.67×10^{2}	3.33×10^{2}	3.10×10^{2}
62,000	9.36×10^{2}	7.96×10^{2}	7.25×10^{2}	6.79×10^{2}
70,000	2.24×10^{3}	1.96×10^{3}	1.80×10^{3}	1.70×10^{3}
80,000°	5.00×10^{3}	4.41×10^{3}	4.09×10^{3}	3.87×10^{3}

negligible, because here the weight function approaches zero. The most serious effect of our neglect of the Gaunt factors is that we have made the continuous absorption coefficient of hydrogen too large just to the violet of the Lyman limit and of the Balmer limit. In practice, however, at the red side of these limits an additional source of pseudo continuous absorption appears owing to the overlap of the wide-spread wings of the higher members of the Lyman and Balmer series. This apparent

continuous absorption is not included in the calculation of the mean continuous absorption coefficient, and its effect on the mean absorption coefficient may be allowed for by neglecting the Gaunt factor. When it is a question of calculating the mono-chromatic continuous absorption coefficient at any wavelength and working with this, we should closely consider the effect of Gaunt factor and the overlap of the wings of the lines. We neglect both these factors in the ensuing computations, consequently the discontinuity we calculate in the continuous absorption coef-ficient at the Lyman and Balmer limits will be larger in our model atmosphere than it would be in an actual stellar atmo-sphere of the same structure. This is because we calculate k_ν too large on the violet side of the limit and too small on the red side. The effects of these approximations on the continuous absorption coefficient of ionised helium are not important for ionised helium is not a major contributor to the opacity of our stellar atmosphere.

To obtain k_ν (*He I*), the monochromatic absorption coefficient for neutral helium per gram of neutral helium corrected for stimulated emission, we must sum the contributions from each of the continua of neutral helium. Atomic absorption coefficients for the continua from the ground level of neutral helium, 1^1S, and from the excited states 2^1S, 2^3S, 2^1P and 2^3P, have been published. However, no value of the atomic absorption coefficient for levels with $n \geq 3$ are available. In order to evaluate the

Table 3.

The continua of the *He I* atom.

Level	E. P.	λ limit	source for a_ν
1^1S	0.00 V	504 A	S. HUANG, Ap. J. **108**, 354, 1948.
2^3S	19.73	2601	
2^1S	20.53	3112	
2^3P	20.87	3436	L. GOLDBERG, Ap. J. **90**, 414, 1939, for the P-D continua and approximate formulae, privately communicated, for the P-S continua.
2^1P	21.13	3682	
$n=3$	22.88	7710	hydrogen-like formulae.
$n=4$	23.60	14,020	
$n=5$	23.92 V	22,030 A	

contribution to the monochromatic absorption coefficient from the continua arising from these levels and from the free-free transitions we assume the helium atom is hydrogen-like, and that Kramer's law can be used. Information about the position of the various series limits and the sources we shall use for a_ν, the atomic absorption coefficient, is given in Table 3. Mean excitation potentials are given for the levels with $n = 3$, 4 and 5.

The contribution to k_ν (He I) from any one continuum is $a_\nu \times$ number of atoms in the appropriate level. We assume the excitation is according to Boltzman's law, hence

$$\frac{n_{n,s}}{n_r} = \frac{g_{r,s}}{u_r} e^{-\chi_{r,s}/kT}$$

where $n_{n,s}$ is the number of atoms in the rth state of ionisation excited to the state s which has an excitation energy $\chi_{r,s}$. As usual n_r is the total number of atoms in the rth stage of ionisation, $g_{r,s}$ is the statistical weight of the level s, and u_r is the partition function. We wish to find k_ν (He I) per gram of neutral helium, hence $n_r = 1/m_{He}$, where m_{He} is the mass of the helium atom. At any temperature T, the contribution from level s to k_ν (He I), corrected for stimulated emission, is

$$k_\nu(s) \frac{g_{1,s}}{m_{He}} e^{-\chi_{1,s}/kT} a_\nu(s) (1 - e^{-h\nu/kT}), \qquad (24)$$

since the partition function for neutral helium is unity. Here $a_\nu(s)$ is the atomic absorption coefficient at frequency ν in the continuum arising from level s. The atomic absorption coefficient, a_ν, for the continua from the 1^1S, 2^1S and 2^3S levels can be found from tables given by HUANG (14). We shall use a mean of the values given by Huang for the dipole moment and the momentum interaction. The atomic absorption coefficient for the continua occurring at the limits of the $2^1P - n^1D$ and $2^3P - n^3D$ series can be read from a graph given by GOLDBERG (15), or computed from the formulae he gives. Dr. Goldberg has privately communicated to me the following approximate formulae for the atomic absorption coefficients in the continua arising at the heads of the $2^1P - n^1S$ and $2^3P - n^3S$ series. In the continuum at the head of the $2^1P - n^1S$ series,

$$a_\nu \sim \frac{1}{2R} \frac{\pi e^2}{mc} 10^{-15 \cdot 71} \nu_{n'}^{4 \cdot 6} \nu^{-3 \cdot 6},$$

and in the continuum at the head of the $2^3P - n^3S$ series

$$a_\nu \sim \frac{1}{2R} \frac{\pi e^2}{mc} 10^{-15 \cdot 80} \nu_{n'}^{4 \cdot 3} \nu^{-3 \cdot 3}.$$

Here R is the Rydberg constant in frequency units, $\nu_{n'}$ is the frequency of the series limit, and ν is the frequency at which we wish to find the atomic absorption coefficient. When the numerical factors are introduced we have at the head of the $2^1P - n^1S$ series

$$\log a_\nu = 35 \cdot 48 - 3 \cdot 6 \log \nu \qquad (25)$$

and at the head of the $2^3P - n^3S$ series

$$\log a_\nu = 31 \cdot 06 - 3 \cdot 3 \log \nu. \qquad (26)$$

To find the contributions to $k_\nu (He\ I)$ from levels with $n \geq 3$ and from the free-free transitions we must consider the helium atom to be hydrogen-like. According to Kramers law the absorption coefficient per neutral atom at frequency ν for a bound-free transition is

$$a_\nu(n, \infty) = \frac{64\pi^4}{3\sqrt{3}} \frac{Z_{\text{eff}}^4 e^{10} m}{ch^6} \frac{e^{-u_1}}{\nu^3} \sum' \frac{e^{u_n}}{n^3}, \qquad (27)$$

for a hydrogen-like atom of effective nuclear charge Z_{eff}. The summation is carried out over all continua with limits to the red of the frequency being considered. As in the discussion for hydrogen and ionised helium, u_n is the quantity $h\nu_n/kT$, where ν_n is the frequency of the series limit n. The absorption coefficient per neutral helium atom at frequency ν due to free-free transitions is

$$a_\nu(\infty, \infty) = \frac{64}{3\sqrt{3}} \frac{\pi^4 e^{10} m}{ch^6} \frac{2 e^{-u_1}}{u_1} \frac{1}{\nu^3} \qquad (28)$$

since although for free-free transitions $Z_{\text{eff}} = 1$ as in hydrogen, the ratio of the partition functions is $^2/_1$ instead of $^1/_2$ as for hydrogen. Upon combining equations (27) and (28) and in-

tegrating the terms of the sum in equation (27) for values of $n > 5$ (cf. Unsöld [12] p. 118), we obtain for the absorption coefficient per atom of neutral helium

$$a_\nu(He\,I, n \geq 3) =$$

$$= \frac{64\,\pi^4\,e^{10}\,m}{3\,\sqrt{3}\,ch^6}\frac{e^{-u_1}}{\nu^3}\left[Z_{\text{eff}}^4\left\{\sum_{3 \leq n}^{5}{}'\frac{e^{u_n}}{n^3} + \frac{(e^{u_5}-1)}{2\,u_1}\right\} + \frac{2}{u_1}\right]. \quad\quad (29)$$

The absorption coefficient per gram of neutral helium corrected for stimulated emission is

$$k_\nu(He\,I, n \geq 3) = \frac{1}{m_{He}}\,a_\nu(He\,I, n \geq 3)\,(1 - e^{-h\nu/kT}). \quad (30)$$

The total absorption coefficient at any frequency ν of neutral helium per gram of neutral helium corrected for stimulated emission is the sum of the contributions from the individual continua with $n \leq 2$ (eq. [24]), and the contribution from the levels with $n > 3$, and from the free-free transitions (eq. [30]).

We must now determine Z_{eff} for the levels $n \geq 3$ of $He\,I$. For a hydrogen-like level

$$Z_{\text{eff}}^2 = n^2\,(R\lambda_n)^{-1} \quad\quad (31)$$

where R is the Rydberg constant, $1\cdot097 \times 10^5\,\text{cm}^{-1}$, and λ_n is the wavelength of the series limit n. We have given λ_n in Table 3 for the levels $n = 3$, 4 and 5. From equation (31) we find for $n = 3$, 4 and 5, $Z_{\text{eff}} = 1\cdot032$, $1\cdot019$ and $1\cdot017$ respectively. The mean value of Z_{eff} is 1.023. Since only the levels with $n = 3$, 4 and 5 contribute appreciably to the continuous absorption in the wavelength region in which we are interested, we use the Z_{eff} which gives a mean representation of the energies of these levels.

We have now shown how to obtain $k_\nu(H)$, $k_\nu(He\,I)$ and $k_\nu(He\,II)$ at any temperature corrected for stimulated emission. In this connection it may be remarked that, as Rudkjøbing has shown (8), the coefficient of electron scattering should not be

multiplied by the factor $(1 - e^{-h\nu/kT})$. With this information we can readily find $\bar{k}(H)$, $\bar{k}(He\ I)$ and $\bar{k}(He\ II)$ as functions of the temperature and hence of the optical depth, for the weight functions are tabulated, (9) or (11), as functions of the optical depth.

To obtain the structure of the atmosphere we must integrate the equation of mechanical equilibrium, equation (10), step by step. Since from equations (12), (19), (20) and (21) we can obtain $\bar{\varkappa} + \sigma$ as a function of the election pressure and the optical depth, it is convenient to express p_g in term of p_e and work with τ as the independent variable and p_e as the dependent variable. We have

$$\frac{p_g}{p_e} = \frac{N_H(1 + x_H) + N_{He}(1 + x_{He\ I} + 2\ x_{He\ II})}{N_H x_H + N_{He}(x_{He\ I} + 2\ x_{He\ II})}$$

or inserting numerical values

$$\frac{p_g}{p_e} = \frac{0\cdot585\,(1 + x_H) + 0\cdot104\,(1 + x_{He\ I} + x_{He\ II})}{0\cdot585\,x_H + 0\cdot104\,(x_{He\ I} + 2\ x_{He\ II})}. \qquad (32)$$

However, for the values of T and p_e of interest in the outer part of the atmosphere p_g/p_e is very close to 2. Hence we explicitly assume $p_g = 2\,p_e$, and find the structure of our atmosphere by integrating numerically the equation

$$\frac{dp_e}{d\tau} = \frac{1}{2}\left[\frac{g}{\bar{\varkappa} + \sigma} - \frac{\sigma_R}{c}\,T_e^4\right]. \qquad (33)$$

The presence of the term $(\sigma_R/c)\,T_e^4$ in equation (33) shows that $dp_e/d\tau$ may become quite small. Consequently $dp_g/d\tau$ will become small. If such is the case, convection will set in, for K. Schwarzschild has shown that if the existing temperature and pressure gradients are such in an atmosphere that

$$\left|\frac{d\log T}{d\log p_g}\right| > \left|\left(\frac{d\log T}{d\log p_g}\right)_{\text{ad}}\right|$$

convection will occur. The existing gradient at any level in the atmosphere may be found from

$$\frac{d \log T}{d \log p_g} = \frac{p_g}{T}\left(\frac{dp_g}{d\tau}\right)^{-1}\frac{dT}{d\tau}, \tag{34}$$

and the adiabatic gradient from

$$\left(\frac{d \log T}{d \log p_g}\right)_{ad} = \frac{4(B+1)\,p_r/p_g + \left[1 + B\,(5/2 + \chi_1/kT)\right]}{4(A+4)\,p_r/p_g + \left[5/2 + A\,(5/2 + \chi_1/kT)\right]} \tag{35}$$

which gives the adiabatic gradient for a mixture of radiation and an ionisable gas, one component of which is being ionised, in thermodynamic equilibrium at temperature T, (10). Here we have

$$p_r = \frac{1}{3}\,a\,T^4$$

where a is the Stefan-Boltzman constant, $7 \cdot 55 \times 10^{-15}$ ergs/cm^3/degree^4. In equation (35) χ_1, is the ionisation energy of the element being ionised,

$$B = \nu_1\left[\frac{1+\bar{x}}{x_1\,(1-x_1)} + \frac{\nu_1}{\bar{x}}\right]^{-1}$$

and

$$A = B\,(5/2 + \chi_1/kT),$$

where ν_1 is the relative abundance by number of the element being ionised, x_1 is the degree of ionisation of this element, and $\bar{x}$ is the mean degree of ionisation,

$$\bar{x} = \sum \nu_i\,x_i.$$

A comparison of the results from equations (34) and (35) will show at what depths convection sets in.

In the convective zone the actual temperature gradient will be greater than the adiabatic gradient and less than the radiative gradient, and its exact value will depend upon the relative importance of radiative transport of energy to convective transport. We shall see that in our model the adiabatic gradient is very much the same as the radiative gradient, hence in the convective zone we shall find the structure of our model, that is

the dependence of temperature on pressure, by integrating equation (35). In doing this we do not assume $p_g = 2\,p_e$, but use the exact relation

$$p_g/p_e = (1 + \bar{x})/\bar{x}.$$

The use of equation (35) implies that the radiation field at any level in the atmosphere is that for an enclosed volume in thermodynamic equilibrium at temperature T. Since the convective zone is at some depth in the atmosphere, this approximation is valid. We continue to assume the existence of a state of local thermodynamic equilibrium for the calculation of the ionisation in the atmosphere at any level, as we have done throughout the atmosphere.

3. The numerical results of the integration of a model atmosphere are given in this section. We start from the boundary conditions that $T_0 = 25{,}200°$ and $p_e = 0$, and integrate equation (33) inwards step by step. In the region $0 < \tau < 0{\cdot}10$ we use steps of $\varDelta\tau = 0{\cdot}01$, in the region $0.10 < \tau < 1.0$ we use $\varDelta\tau = 0{\cdot}10$, and from $1.0 < \tau < 3{\cdot}0$ we use $\varDelta\tau = 0{\cdot}20$. In order to find

$$\varDelta\,p_e = \frac{1}{2}\left[\frac{g}{\bar{\varkappa} + \sigma} - \frac{\sigma_R}{c}\,T_e^4\right]\varDelta\tau$$

at any level τ we must know p_e and T at the level τ. The value of T can be found from equation (12) and the value of p_e is found by trial so that

$$\frac{1}{2}\left(\varDelta p_{e_{\tau-\varDelta\tau}} + \varDelta p_{e_\tau}\right) = p_{e_\tau} - p_{e_{\tau-\varDelta\tau}}$$

where $\varDelta p_{e_{\tau-\varDelta\tau}}$ is the increment in p_e calculated at the level $\tau - \varDelta\tau$, $\varDelta p_{e_\tau}$ is the increment in p_e calculated with the assumed p_e at level τ, and $p_{e_{\tau-\varDelta\tau}}$ is the value of the electron pressure at the level $\tau - \varDelta\tau$. We take $\log g = 4{\cdot}200$ and we use the value $T_e = 30{,}000°$ which is consistent with the use of the temperature law given in equation (12) and our boundary temperature of $25{,}200°$. The quantities $\bar{k}\,(H)$, $\bar{k}\,(He\,I)$ and $\bar{k}\,(He\,II)$ (cf. eq. [19] and [20]) were computed at the levels $\tau = 0{\cdot}0$, $0{\cdot}20$, $0{\cdot}50$, $1{\cdot}00$, $1{\cdot}40$,

2.00 and graphical interpolation was used to get the $\bar{k}$'s at other optical depths. We used the weight functions tabulated by CHANDRASEKHAR (9) to form the $\bar{k}$'s although strictly speaking this procedure is not quite correct (cf. [11]). We felt justified in doing this because preliminary computations showed that the quantity $\lambda = \bar{\varkappa}/(\bar{\varkappa} + \sigma)$ would be close to unity, and under these circumstances the weight functions tabulated by Chandrasekhar are preferable to those which allow for the effect of electron scattering (11), but make a rather restrictive assumption about the dependence of the Plank function on optical depth. The graphs of the $\bar{k}$'s were extrapolated linearly to $\tau = 3 \cdot 0$, and the model was integrated to this depth step by step. The model atmosphere found is given in Table 4. Log p_g is tabulated rather than log p_e. It will be recalled that we have assumed $p_g = 2\,p_e$ in this region, and that $\theta = 5040/T$.

Table 4.

A model atmosphere with $T_0 = 25,200°$, log $g = 4 \cdot 200$: Radiative zone.

τ	θ	log p_g	$\bar{\varkappa}$	σ	τ	θ	log p_g	$\bar{\varkappa}$	σ
0.00	0.200	2.121	0.802	0.274	0.60	0.170	3.301	3.418	0.275
.01	.199	2.377	1.396	.274	0.70	.167	3.357	3.447	.276
.02	.199	2.489	1.798	.274	0.80	.164	3.407	3.447	.276
.03	.198	2.563	2.033	.274	0.90	.162	3.450	3.526	.277
.04	.197	2.619	2.217	.274	1.00	.159	3.490	3.417	.278
.05	.197	2.665	2.467	.274	1.20	.154	3.549	3.167	.280
.06	.196	2.702	2.568	.274	1.40	.150	3.619	3.136	.282
.07	.195	2.736	2.671	.274	1.60	.147	3.679	3.230	.284
.08	.194	2.765	2.730	.274	1.80	.144	3.731	3.220	.287
.09	.194	2.791	2.896	.274	2.00	.141	3.777	3.168	.290
.10	.193	2.814	2.916	.274	2.20	.139	3.818	3.224	.292
.20	.187	2.926	2.922	.274	2.40	.137	3.856	3.241	.294
.30	.182	3.066	3.253	.274	2.60	.134	3.892	3.070	.297
.40	.178	3.162	3.428	.275	2.80	.132	3.926	3.041	.299
0.50	0.174	3.237	3.467	0.275	3.00	0.131	3.958	3.142	0.300

We must now test this model for stability against convection by computing the radiative gradient $(d \log T/d \log p_g)_{rad}$ from

equation (34) and comparing it with the adiabatic gradient $(d \log T/d \log p_g)_{ad}$ at the same temperature and pressure calculated according to equation (35). The results of these calculations are given in Table 5. We see that the atmosphere becomes convectively unstable at about $\tau = 2 \cdot 00$ or $\theta = 0 \cdot 141$. Since the difference between the radiative gradient and the adiabatic gradient is not large, we do not expect any large scale disturbances to occur as a result of the setting in of convection at these levels.

Table 5.

The temperature—pressure gradients in the radiative zone.

τ	$\left(\dfrac{d \log T}{d \log p_g}\right)_{rad}$	$\left(\dfrac{d \log T}{d \log p_g}\right)_{ad}$	τ	$\left(\dfrac{d \log T}{d \log p_g}\right)_{rad}$	$\left(\dfrac{d \log T}{d \log p_g}\right)_{ad}$
1.00	0.168	0.230	2.40	0.197	0.188
1.40	0.161	0.200	3.00	0.201	0.197
2.00	0.183	0.188	..	..	..

In order to obtain the structure of the atmosphere at greater depths, higher temperatures, we assume an adiabatic temperature gradient and proceed by integrating equation (35). We assume the ionisation of hydrogen and the first ionisation helium to be complete, and we compute x_1, the second degree of ionisation of helium, from the equation.

$$\log \frac{x_1}{1-x_1} = -54 \cdot 14\,\theta + \frac{5}{2} \log T - 0 \cdot 477 - \log p_e.$$

We note that in this approximation the mean degree of ionisation is

$$\bar{x} = 1 \cdot 00 + 0 \cdot 15\,x_1$$

since the abundance by number of helium is $0 \cdot 15$. The resulting model atmosphere is given in Table 6. Here the assumption $p_g = 2\,p_e$ is not made, and the quantity $\bar{z}$ is not defined.

The model atmosphere given in Tables 4 and 6 may be compared with the model atmosphere with $\theta_0 = 0 \cdot 20$ and log

Table 6.

A model atmosphere with $T_0 = 25{,}200^\circ$, $\log g = 4{\cdot}200$:
Convective zone.

θ	$\log p_g$	$\log p_e$	σ	θ	$\log p_g$	$\log p_e$	σ
0.131	3.958	3.657	0.300	0.0947	4.558	4.286	0.315
.125	4.058	3.780	.305	.0886	4.658	4.386	.315
.119	4.158	3.882	.309	.0830	4.758	4.486	.315
.113	4.258	3.984	.312	.0779	4.858	4.586	.315
.107	4.358	4.085	.313	.0730	4.958	4.686	.315
0.101	4.458	4.186	0.314	.0685	5.058	4.786	.315
..	..	..	..	0.0642	5.158	4.986	0.315

$g_{\text{eff}} = 4{\cdot}20$ computed by Rudkjøbing (8). Rudkjøbing computes the structure of his model using an effective acceleration of gravity, and goes on to estimate that the true acceleration of gravity of his model is $10^{4{\cdot}26}$. In computing our model we have assumed that the actual acceleration of gravity is $10^{4{\cdot}20}$, however, a rough comparison of our models may be made. In the outermost regions of both atmospheres the run of gas pressure with temperature is about the same, but the gas pressure begins to increase more rapidly with increasing temperature in Rudkjøbing's model than in ours and at moderate depths, $\theta \sim 0{\cdot}17$, the gas pressure in Rudkjøbing's model is about 16 percent larger than in the present model. Rudkjøbing finds that convection starts at about the same level, $\theta \sim 0{\cdot}141$, as in the present model atmosphere.

In assessing the behaviour of our model atmosphere it is of interest to find the run with depth of $\log g_{\text{eff}}$, obtained from equations (9) and (11), the quantity $\lambda = \bar{\varkappa}/(\bar{\varkappa} + \sigma)$, the ratio p_g/p_e computed according to equation (32), and the ratio p_r/p_g. We obtain the radiation pressure at any depth τ by integrating the equation, (cf. eq. [9]),

$$\frac{dp_r}{d\tau} = \frac{\sigma_R}{c} T_e^4$$

under the boundary condition that p_r is zero at $\tau = 0$. An

Table 7.

Values of certain quantities in the model atmosphere:
Radiative zone.

τ	$\log g_{\text{eff}}$	λ	p_g/p_e	p_r/p_g	$\bar{\varkappa}(H)$	$\bar{\varkappa}(He\,I)$	$\bar{\varkappa}(He\,II)$
0.00	4.152	0.745	1.998	0.000	0.433	0.386	0.001
0.05	4.068	.900	2.000	.166	1.377	1.087	.003
0.10	4.041	.914	2.000	.235	1.690	1.222	.004
0.40	4.009	.926	1.997	.422	2.183	1.228	.017
0.80	4.009	.926	1.991	.480	2.302	1.088	.057
1.20	4.025	.919	1.979	.519	2.144	0.893	.130
1.60	4.017	.919	1.964	.513	2.151	0.808	.271
2.00	4.025	.916	1.945	.512	2.156	0.625	.387
3.00	4.025	0.913	1.913	0.506	2.287	0.373	0.482

abridged table of these quantities is given in Table 7. Also given
in Table 7 are $\bar{\varkappa}(H)$, $\bar{\varkappa}(He\,I)$, $\bar{\varkappa}(He\,II)$ the contributions of
hydrogen, neutral helium, and ionised helium respectively to the
mean absorption coefficient, $\bar{\varkappa}$.

In the convective zone the ratios p_g/p_e and p_r/p_g can be
found directly from their definitions. The value of the effective
acceleration of gravity is found from the following considerations.
We postulate that the model atmosphere must still be in mechanical
equilibrium in the convective zone. Consequently we require

$$\frac{dp_g}{dz} + \frac{dp_r}{dz} = -g\,\varrho \tag{36}$$

in addition to the condition that $d\log T/d\log p_g$ is adiabatic,
equation (35). Since in the convective zone we assume that the
radiation field is that for an enclosed volume in thermodynamic
equilibrium at temperature T we have

$$\frac{dp_r}{dz} = \frac{4}{3}\,aT^3\frac{dT}{dz}.$$

However

$$\frac{dT}{dz} = \frac{T}{p_g}\left(\frac{d\log T}{d\log p_g}\right)_{\text{ad}}\frac{dp_g}{dz},$$

hence we find

$$\frac{dp_r}{dz} = \frac{4}{3}\,\frac{aT^4}{p_g}\left(\frac{d\log T}{d\log p_g}\right)_{\text{ad}}\frac{dp_g}{dz}.$$ (37)

Remembering that

$$p_r = \frac{1}{3}\,aT^4$$

and introducing equation (37) into equation (36), we obtain.

$$\frac{dp_g}{dz}\left[1 + 4\,\frac{p_r}{p_g}\left(\frac{d\log T}{d\log p_g}\right)_{\text{ad}}\right] = -g\varrho.$$ (38)

It follows that

$$g_{\text{eff}} = g\left[1 + \frac{4\,p_r}{p_g}\left(\frac{d\log T}{d\log p_g}\right)_{\text{ad}}\right]^{-1}.$$ (39)

The values for $\log g_{\text{eff}}$ given in Table 8 were found from equation (39).

From Tables 7 and 8 we see that the effective acceleration of gravity varies with depth in the atmosphere and that the radiation pressure is an appreciable fraction of the gas pressure except in the outermost layers of the stellar atmosphere. Consequently radiation pressure and its effects can not be neglected in an atmosphere such as this. In most of the radiative zone the

Table 8.

Values of certain quantities in the model atmosphere: Convective zone.

θ	$\log g_{\text{eff}}$	P_g/P_e	P_r/P_g	θ	$\log g_{\text{eff}}$	P_g/P_e	P_r/P_g
0.131	4.025	1.91	0.506	0.0947	3.989	1.87	0.552
.125	4.024	1.90	.580	.0886	3.982	1.87	.580
.119	4.016	1.89	.558	.0830	3.978	1.87	.595
.113	4.009	1.88	.542	.0779	3.973	1.87	.601
.107	4.002	1.88	.542	.0730	3.968	1.87	.630
0.101	3.990	1.87	0.548	.0685	3.964	1.87	.648
..	..	..	..	0.0642	3.959	1.87	0.665

ratio p_g/p_e is close to the assumed value of 2·0, but near the beginning of the convective zone this ratio decreases. This is because at the temperatures and pressures of these layers the second ionisation of helium is becoming important. In the radiative zone the quantity λ is sufficiently close to unity to justify the use of CHANDRASEKHAR's weight functions for forming $\bar{x}$, cf. (11). We see that at all depths hydrogen is the main contributor to the opacity. Neutral helium is an important contributor in the outer regions but at greater depths the second ionisation of helium sets in and then neutral helium decreases in importance as a source of opacity while ionised helium increases in importance. In the convective zone we have assumed that the ionisation of hydrogen and the first ionisation of helium are complete. At the level $\tau = 3·0$ we have $1 - x_H = 2·77 \times 10^{-6}$ and $N_{\text{He}^+}/N_{He^0} = 5·36 \times 10^4$, hence these assumptions are justified.

4. We have constructed a model atmosphere in mechanical equilibrium and we must now compute the net flux at various levels and see if this flux is constant with depth. If this is so we may say that our model atmosphere represents a real stellar atmosphere. The following method of computing the net flux at any level in the atmosphere has been developed by STRÖMGREN (16). The monochromatic equation of transfer for a stellar atmosphere in which the opacity is given by continuous absorption and by electron scattering is

$$\cos\vartheta \frac{dI_\nu}{dt_\nu} = I_\nu - S_\nu \tag{40}$$

where t_ν is the monochromatic optical depth

$$t_\nu = -\int (\varkappa_\nu + \sigma)\,\varrho\,dz, \tag{41}$$

and S_ν is the source function,

$$S_\nu = \lambda_\nu\,B_\nu + (1 - \lambda_\nu)\,J_\nu, \tag{42}$$

where

$$\lambda_\nu = \varkappa_\nu/(\varkappa_\nu + \sigma)$$

and
$$J_\nu = \frac{1}{2} \int_0^\pi I_\nu \sin \vartheta \, d\vartheta .$$

We have

$$J_\nu(t_\nu) = \frac{1}{2} \int_{t_\nu}^\infty S_\nu(t_\nu') K_1(t_\nu' - t_\nu) \, dt_\nu' + \frac{1}{2} \int_0^{t_\nu} S_\nu(t_\nu') K_1(t_\nu - t_\nu') \, dt_\nu' \quad (43)$$

where K_1 is the first exponential integral. If we introduce equation (42) into equation (43) and also define the quantity

$$Y_\nu = J_\nu - B_\nu, \tag{44}$$

we obtain the following functional equation for $Y_\nu(t_\nu)$,

$$\left. \begin{aligned} Y_\nu(t_\nu) &= -B_\nu(t_\nu) + \frac{1}{2} \int_0^\infty B_\nu(t_\nu') K_1(|t_\nu' - t_\nu|) \, dt_\nu' \\ &\quad + \frac{1}{2} \int_0^\infty [1 - \lambda_\nu(t_\nu')] \, Y_\nu(t_\nu) K_1(|t_\nu' - t_\nu|) \, dt_\nu' . \end{aligned} \right\} \tag{45}$$

We now define

$$\overline{B_\nu(t_\nu)} = \frac{1}{2} \int_0^\infty B_\nu(t_\nu') K_1(|t_\nu' - t_\nu|) \, dt_\nu'$$

and find $Y_\nu(t_\nu)$ by an iterative process which gives

$$Y_\nu(t_\nu) = Y_\nu^0(t_\nu) + \varDelta^1 Y_\nu + \varDelta^2 Y_\nu + \cdots$$

where

$$Y_\nu^0(t_\nu) = \overline{B_\nu(t_\nu)} - B_\nu(t_\nu), \tag{46}$$

$$\varDelta^1 Y_\nu = \frac{1}{2} \int_0^\infty [1 - \lambda_\nu(t_\nu')] \, Y_\nu^0(t_\nu') K_1(|t_\nu' - t_\nu|) \, dt_\nu', \tag{47}$$

$$\varDelta^2 Y_\nu = \frac{1}{2} \int_0^\infty [1 - \lambda_\nu(t_\nu')] \, \varDelta^1 Y_\nu(t_\nu') K_1(|t_\nu' - t_\nu|) \, dt_\nu', \tag{48}$$

and in general

$$\varDelta^n Y_\nu = \frac{1}{2} \int_0^\infty [1 - \lambda_\nu(t_\nu')] \, \varDelta^{n-1} Y_\nu(t_\nu') K_1(|t_\nu' - t_\nu|) \, dt_\nu'.$$

If the $\Delta^n Y_\nu$ very nearly form a series of constant ratio $(1 - \lambda_\nu)$, we can write

$$Y_\nu(t_\nu) = Y_\nu^0(t_\nu) + \Delta^2 Y_\nu + \lambda_\nu^{-1} \Delta^2 Y_\nu \tag{49}$$

as an approximation. This approximation is quite good when λ_ν is not very small. When λ_ν is small it is better to extend the series to at least $\Delta^3 Y_\nu$ or $\Delta^4 Y_\nu$ before attempting a summation of the remaining correction terms. It follows from equations (44) and (42) that the source function at any level t_ν is

$$S_\nu(t_\nu) = B_\nu(t_\nu) + \left[1 - \lambda_\nu(t_\nu)\right] \left[Y_\nu^0(t_\nu) + \Delta^2 Y_\nu + \lambda_\nu^{-1} \Delta^2 Y_\nu\right], \tag{50}$$

and that the net flux at this level t_ν is given by

$$F_\nu(t_\nu) = 2 \int_{t_\nu}^{\infty} S_\nu(t_\nu') K_2(t_\nu' - t_\nu) \, dt_\nu' - 2 \int_0^{t_\nu} S_\nu(t_\nu') K_2(t_\nu - t_\nu') \, dt_\nu', \tag{51}$$

where K_2 is the second exponential integral. The integrations over the exponential integrals occurring in equations (46), (47), (48), and (51) may be performed by a method of representative points and weights developed by Strömgren (17).

We see that to obtain the source function at any depth we must know the dependence of the Planck function B_ν on t_ν.

Since
$$dt_\nu = \frac{\varkappa_\nu + \sigma}{\varkappa + \sigma} d\tau \tag{52}$$

we may find t_ν as a function of τ, and thus of temperature, by integrating equation (52) numerically. With this information we can construct tables giving $B_\nu(t_\nu)$. In the convective zone, however, the optical depth, τ, is not defined and the following device must be used to obtain t_ν as a function of temperature. By definition

$$\frac{dt_\nu}{dz} = -(\varkappa_\nu + \sigma)\varrho$$

hence from equation (38) we obtain

$$\frac{dt_\nu}{dp_g} = \frac{\varkappa_\nu + \sigma}{g}\left[1 + \frac{4\,p_r}{p_g}\left(\frac{d\log T}{d\log p_g}\right)_{\mathrm{ad}}\right]$$

or
$$dt_\nu = \frac{\varkappa_\nu + \sigma}{g}\left[1 + \frac{4\,p_r}{p_g}\left(\frac{d\log T}{d\log p_g}\right)_{\mathrm{ad}}\right]p_g\,d\,(\log p_g).\qquad(53)$$

Equation (53) may be integrated numerically to give t_ν as a function of $\log p_g$ and hence of temperature, since in the convective zone we use $\log p_g$ as the independent variable. Using equations (52) and (53) we obtained $B_\nu(t_\nu)$ at a number of wavelengths and then computed tables of $S_\nu(t_\nu)$ according to equation (50). From these tables of the monochromatic source function the net monochromatic flux at any level is readily obtained by evaluating equation (51) by means of STRÖMGREN's tables of representative points and weights (17). I was greatly privileged to use these tables before publication. Without these tables it would have been impossible to have done this work.

We wish to ascertain if the integrated flux

$$F = \int_0^\infty F_\nu\,d_\nu$$

is constant with depth. In order to perform this integration over frequency we divide the continuous spectrum into four regions, $\lambda\,504$, the $1\,^1S$ limit of $He\,I$, to $\lambda\,912$; $\lambda\,912$ to $\lambda\,1458$; $\lambda\,1458$ to $\lambda\,3646$; $\lambda\,3646$ to $\lambda\,8204$, the Paschen limit of H. The integrated flux in each of these intervals is obtained by finding F_ν at five points equidistant in frequency and summing with the appropriate weights using COTES' formula. The selected wavelengths and the monochromatic fluxes at the depths $\tau = 0.0, 0.10, 0.60,$ and 1.00 are given in Table 9. The last line of the table gives the integrated net flux, $F(\tau)$, at each level. The emergent flux in the region $\lambda\,228$, the Lyman limit of $He\,II$, to $\lambda\,504$ was calculated for the level $\tau = 0$, but it was found to be negligible, hence the computations for this region were not carried through to obtain F_ν at other optical depths. Likewise we neglect the flux to the red of the Paschen limit. This flux contributes a very small part to the total flux, and its neglect will not affect our determination of the effective temperature or of the constancy of F with depth.

The mean flux is $F = 33\cdot29 \times 10^{12}$ ergs/cm²/sec which corresponds to an effective temperature of $36{,}800°$. The deviations

Table 9.

The monochromatic flux, F_ν, in the model atmosphere.

λ	$\tau = 0.0$	$\tau = 0.10$	$\tau = 0.60$	$\tau = 1.00$
504.3 r	8.05×10^{-4}	9.00×10^{-4}	1.40×10^{-3}	1.69×10^{-3}
567.8	8.42	9.28	1.36	1.72
649.4	8.79	9.64	1.31	1.75
758.7	10.96	11.51	1.31	1.61
911.6 v	15.41×10^{-4}	13.17×10^{-4}	1.20×10^{-3}	1.42×10^{-3}
911.6 r	18.87×10^{-3}	18.48×10^{-3}	18.48×10^{-3}	19.30×10^{-3}
1006	18.18	18.11	18.69	19.01
1122	16.02	16.19	16.69	17.27
1268	14.06	14.01	14.06	14.41
1458	11.69×10^{-3}	11.68×10^{-3}	11.79×10^{-3}	11.77×10^{-3}
1458	11.69×10^{-3}	11.68×10^{-3}	11.79×10^{-3}	11.77×10^{-3}
1716	9.55	9.50	9.33	9.62
2083	7.82	7.81	7.67	7.36
2652	5.47	5.37	5.07	4.68
3646 v	3.41×10^{-3}	3.32×10^{-3}	2.82×10^{-3}	2.36×10^{-3}
3646 r	4.02×10^{-3}	4.02×10^{-3}	3.73×10^{-3}	3.48×10^{-3}
4234	3.01×10^{-3}	2.97×10^{-3}	2.70×10^{-3}	2.44×10^{-3}
5048	2.20×10^{-3}	2.30×10^{-3}	1.87×10^{-3}	1.58×10^{-3}
6251	1.48×10^{-3}	1.43×10^{-3}	1.11×10^{-3}	8.53×10^{-4}
8204 v	8.84×10^{-4}	8.24×10^{-4}	5.22×10^{-4}	3.26×10^{-4}
F	32.72×10^{12}	32.67×10^{12}	33.27×10^{12}	34.49×10^{12}

The units of F_ν are ergs/cm²/sec.

from the mean are -1.7, -1.9, 0.0 and $+3.6$ percent respectively at the levels $\tau = 0.00$, 0.10, 0.60 and 1.00. Thus the constancy of the net flux with increasing depth is highly satisfactory in our model. This result vindicates the use of the straight mean absorption coefficient recommended by Chandrasekhar and the treatment of the effects of radiation pressure which we have employed here. The criticism by UNSÖLD (18) of the Chandrasekhar-mean seems hardly to be justified. It is true as Unsöld points out that in the deeper layers where $S_\nu \simeq B_\nu$ the Rosseland-mean and the Chandrasekhar-mean are equivalent and the Rosseland-mean may be preferred because of the ease of forming

Table 10.

Some values of $(S_\nu - B_\nu)/B_\nu$.

τ	$\lambda 504$ v	$\lambda 759$	$\lambda 1122$	$\lambda 1716$	$\lambda 3646$ v	$\lambda 4234$	$\lambda 8204$ v
0.00	0.000	— 0.004	4.98	+ 0.362	— 0.159	— 0.175	— 0.155
0.50	.000	.001	1.12	+ 0.036	.031	.060	.012
1.00	.000	.000	0.568	— 0.026	.014	.037	.004
1.60	.000	.000	0.289	— 0.032	.005	.021	.001
2.20	.000	.000	0.200	— 0.024	.002	.008	.000
3.00	0.000	— 0.000	0.155	— 0.018	— 0.000	— 0.002	— 0.000

it. However, in the upper layers of the atmosphere $S_\nu \neq B_\nu$ and then the use of the Rosseland-mean is subject to criticism. Equation [50] enable us to compute $S_\nu - B_\nu$ at any layer in the atmosphere. A few values of $(S_\nu - B_\nu)/B_\nu$ are given in Table 10 for interest. We see that over much of the spectrum S_ν deviates appreciably from B_ν at depths $\tau < 0.50$. In the transparent region, $912 < \lambda < 1500$ A, however, the deviation of S_ν from B_ν extends to great depths. Since most of the emergent radiation passes in this region it seems advisable in computing the structure of the model to use a mean absorption coefficient which allows for the difference of S_ν from B_ν. In order to use a Chandrasekhar-type mean the weight functions F_ν/F must be evaluated in some manner. This procedure involves certain assumptions about the process of radiation transfer in the stellar atmosphere. CHAN-DRASEKHAR (9) evaluates $F_\nu^{(1)}/F$ in a certain systematic way; UNSÖLD (18) evaluates these weights in another way. Which way is best, and whether either is better than using the Rosseland-mean can only be proven by model atmosphere computations such as carried through here. The present results support the use of Chandrasekhar's weight functions.

That the flux from the model atmosphere increases slightly with depth is not very significant. This behaviour may be the result of using an adiabatic temperature gradient, which is the minimum gradient expected, in the convective zone. Thereby the flux in the wavelength region $912 < \lambda < 1500$ A, which comes effectively from the convective zone, arises from greater depths than it would if the temperature gradient were larger, for a

decrease of the temperature gradient decreases the mono-
chromatic opacity of the atmosphere. The small percentage
reduction of the net flux in the region $912 < \lambda < 1500$ A neces-
sary to make the net flux perfectly constant could easily be
obtained by increasing the temperature gradient in the con-
vective zone slightly. Such an increase would be accordant with
present concepts of the structure of the convective zone in stellar
atmospheres.

Referring to equation (6) we find that

$$\frac{dp_r}{d\tau} = \frac{\sigma_R}{c} T_e^4 + \frac{\pi}{c} \frac{\bar{\varkappa}}{\bar{\varkappa} + \sigma} \int_0^\infty \delta_\nu F_\nu \, d_\nu \tag{54}$$

where

$$\delta_\nu = (\varkappa_\nu / \bar{\varkappa}) - 1 .$$

We have neglected the last term on the right side of equation
(54) when integrating our model. Furthermore we have put
$T_e = 30,000°$, the value corresponding to the boundary tem-
perature $T_0 = 25,200°$, according to the classical $T - \tau$ relation,
equation (12). We have available the information to evaluate
the term

$$\frac{\pi}{c} \frac{\bar{\varkappa}}{\bar{\varkappa} + \sigma} \int_0^\infty \delta_\nu F_\nu \, d_\nu$$

at several values of τ, and we find that it does not vary much
with depth and that its mean value is $- 2 \cdot 37 \times 10^3$. Using this
value and $T_e = 36,800°$ we find that the mean value of $dp_r/d\tau$
is $1 \cdot 18 \times 10^3$. The value used in our computations was $1 \cdot 53 \times 10^3$.
Fortunately these two quantities are not greatly different. Since

$$g_r = -\frac{1}{\varrho} \frac{dp_r}{dz} = (\bar{\varkappa} + \sigma) \frac{dp_r}{dz}$$

we may readily compute the acceleration due to radiation pres-
sure. At the levels $\tau = 0 \cdot 00$, $0 \cdot 10$, $0 \cdot 60$ and $1 \cdot 00$ it is $1 \cdot 57 \times 10^4$,
$3 \cdot 38 \times 10^3$, 3.99×10^3 and 4.10×10^3 cm/sec^2 respectively. For his
model with $\log g_{\text{eff}} = 4.20$ and $T_0 = 25,200°$, Rudkjøbing
estimates that $g_r = 2.35 \times 10^3$ cm/sec^2. His value is less than ours
and that is why his model differs from the present model. How-
ever, Rudkjøbing's estimate is somewhat uncertain for he neglects
some terms. Rudkjøbing estimates g_r from the alternate expression.

$$g_r = \frac{\pi}{c} \int_0^\infty (\varkappa_\nu + \sigma)\, F_\nu \, d\nu \, .$$

He evaluates the integral[1] by putting

$$g_r + \frac{\pi}{c} (\bar{k}_1 F_1 + \bar{k}_2 F_2),$$

where $\bar{k}_1$ and $\bar{k}_2$ are harmonic mean absorption coefficients formed in the manner of the Rosseland-mean, F_1 is the integrated flux in the region $\nu_0 < \nu < \infty$, and F_2 is the integrated flux in the region $0 < \nu < \nu_0$. Here ν_0 is the frequency of the Lyman limit of hydrogen. His approximation means that he is writing

$$\varkappa_\nu + \sigma = \bar{k}_1 \left[1 + \delta_1 (\nu) \right], \quad \nu_0 < \nu < \infty,$$

$$\varkappa_\nu + \sigma = \bar{k}_2 \left[1 + \delta_2 (\nu) \right], \quad 0 < \nu < \nu_0.$$

and that he is neglecting the terms

$$\frac{\pi}{c} \bar{k}_1 \int_{\nu_0}^\infty \delta_1 (\nu)\, F_\nu\, d\nu + \frac{\pi}{c} \bar{k}_2 \int_0^{\nu_0} \delta_2 (\nu)\, F_\nu\, d\nu \, . \tag{55}$$

It is not clear that these terms may be neglected, for the definition of a Rosseland-type mean absorption coefficient sets no condition on the vanishing of such integrals in the gray-body or any other approximation. In our case where we have used a Chandrasekhar-type mean absorption coefficient, which implies

$$\int_0^\infty \delta_\nu F_\nu^{(1)}\, d\nu = 0$$

($F_\nu^{(1)}$ is the monochromatic flux in the gray-body approximation), we have found that

$$\frac{\pi}{c} \int_0^\infty \delta_\nu F_\nu\, d\nu$$

is fairly large.

Rudkjøbing does not give enough data in his paper for us to evaluate (55) directly. However, if we use the flux computed for our model and the values of $\bar{k}_1$, and $\bar{k}_2$ given by Rudkjøbing we find that at the level where $\theta = 0\cdot170$, $\log p_g = 3\cdot30$, i. e.

[1] Note that Rudkjøbing's F is our πF.

$\tau = 0.60$ in the present model, the neglected term is 3.13×10^2 cm/sec^2. Consequently the g_r estimated by Rudkjøbing should be increased to 2.66×10^3. This means that $\log g$ for his model is 4.27. Considering the real difference in the parameter $\log g$ between Rudkjøbing's and the present model, there seems to be no serious difference between our model atmospheres. In order
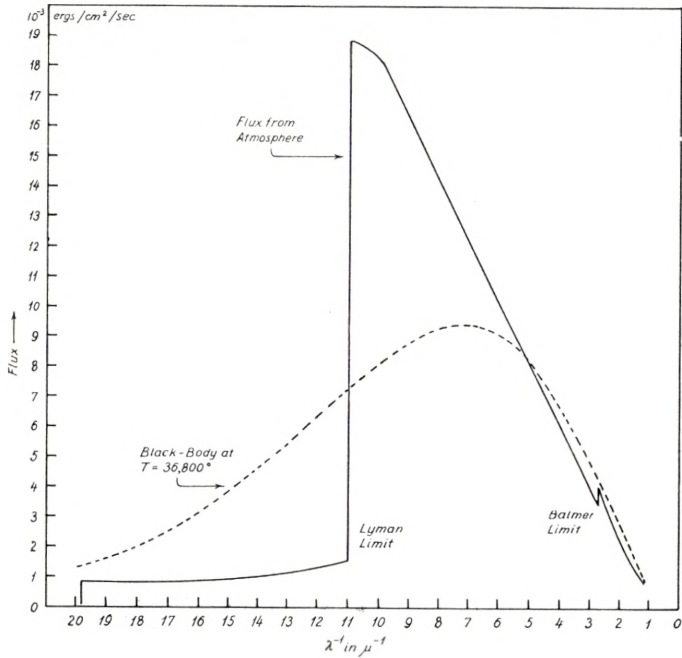

Fig. 1. The emergent flux from the atmosphere as a function of λ^{-1}.

to compute model atmospheres at still higher temperatures and lower surface gravities it would seem preferable to proceed by a method, such as that followed here, which takes account of the effects of radiation pressure directly, rather than the method used by Rudkjøbing, for in these atmospheres the effects of radiation pressure will be important.

The emergent flux is plotted in figure 1 together with B_ν for $T = 36,800^\circ$. We see that in the transparent region of the spectrum, $912 < \lambda < 1500$ A, the emergent flux is greatly in excess of the black-body flux, while in the region beyond the Lyman limit the emergent flux is considerably less than that of a black-body at the effective temperature of the star. In the

visual and photographic regions the emergent flux is less than
the black-body radiation, but roughly parallels it in intensity
distribution. The gradients at any wavelengths in this region are
of little meaning, for gradient is not a sensitive indicator of
temperature at these high temperatures. The Greenwich gradient,
$\lambda\,4100$—$\lambda\,6500$, of our model corresponds to $T > 150,000°$. The
intensity discontinuities at the Lyman limit, the Balmer limit,
and at $\lambda\,504$ for $\tau = 0\cdot00$, $0\cdot10$, $0\cdot60$ and $1\cdot00$, are given in
Table 11. These discontinuities increase a little with depth.

Table 11.
Discontinuities in the continuous spectrum.

τ	Lyman Limit		Balmer Limit		$\lambda\,504$ Limit	
	$\log\dfrac{F_\mathrm{r}}{F_\mathrm{v}}$	$\varDelta$ mag	$\log\dfrac{F_\mathrm{r}}{F_\mathrm{v}}$	$\varDelta$ mag	$\log\dfrac{F_\mathrm{r}}{F_\mathrm{v}}$	$\varDelta$ mag
		m		m		m
0.00	1.088	2.72	0.072	0.18	0.270	0.68
0.10	1.147	2.87	0.083	0.21	0.704	1.76
0.60	1.187	2.97	0.122	0.30	..	..
1.00	1.135	2.84	0.168	0.42	..	..

We did not calculate the discontinuities at the 2^1S, 2^3S, 2^1P
and 2^3P limits of *He* I. However, this does not mean that small
discontinuities are absent here.

According to the work of BARBIER and CHALONGE (19), the
size of the Balmer discontinuity corresponds to spectral type $B1$.
However, as we have indicated in our discussion of the continuous
absorption coefficient $\varkappa_\nu$, we feel our predicted discontinuities
are too large, and it is probable that the model is of earlier
spectral type than $B1$. Since the Gaunt factor (13) is $0\cdot88$ at
$\lambda\,3646\,\mathrm{v}$, we have made $\varkappa_\nu\,(H)$ 12 percent too large at this wave-
length. When $\varkappa_\nu\,(H)$ is reduced by this amount and the emergent
flux on the violet side of the Balmer limit is recalculated, we
find that $F_{3646\,\mathrm{v}}\,(0)$ is $3\cdot49 \times 10^{-3}$. Consequently we obtain log
$F_\mathrm{r}/F_\mathrm{v} = 0\cdot061$. This corrected value corresponds more nearly to
spectral type $B0$ than the value given in Table 11. If we could
estimate the extra pseudo continuous absorption at $\lambda\,3646\,\mathrm{r}$ due
to overlap of the broad wings of the higher members of the
Balmer series, we could compute a more correct value of $F_{3646\,\mathrm{r}}\,(0)$.

3*

In any case it is evident that our computed value is a maximum value. In comparing our predictions with observation we should also note that the observed quantity D, (cf. BARBIER and CHALONGE [19]), which corresponds to our $\log F_r/F_v$ at the Balmer limit, cannot be so clearly defined as the theoretical quantity. Because of the inherent difficulties in the observation of the quantity D, we should expect the observed value of D to be less than the predicted $\log F_r/F_v$. It seems probable that our model corresponds to about spectral type $B0$.

The observed number of hydrogen lines is an indication of absolute magnitude (20). Since we can compute the electron density at any level in our atmosphere from the election pressure and the temperature, we may readily find n_m, the number of hydrogen lines visible, by the TELLER-INGLIS formula (21). The quantity n_m does not vary rapidly with electron density. If we estimate that the higher members of the Balmer series are formed between the levels $\tau = 0\cdot50$ and $\tau = 1\cdot00$ we find that the Balmer series will break off at n_m about 15. Reference to the determination of n_m in a number of early type stars by MICZAIKA (22) and to the spectral types by MORGAN, KEENAN and KELLMAN (23) for these stars, shows that for spectral types between $O9$ and $B2$, $n_m = 15$ corresponds about to luminosity class V. There is little doubt that our model atmosphere represents a main-sequence star.

5. From the continuous spectrum and the electron density of our model atmosphere we have estimated that the model corresponds to about spectral type $BO\ V$. However, it is desirable to confirm this estimate by computing the line spectrum and comparing it to observation. A comparison of the relative strengths of lines arising from atoms in two stages of ionisation will determine the spectral type of the model atmosphere, and a comparison of the absolute strengths of the lines will enable us to derive the abundances of the elements forming the lines. The most prominent lines in the O and B type stars are those from H, $He\,I$ and $He\,II$. These lines are generally used in classifying the spectra of the earliest type stars (4, 23). However, these lines are strongly affected by Stark effect and the adequate representation of their line-absorption coefficients in a stellar atmosphere is a complex problem. Since it would take a separate lengthy investigation to obtain a detailed form for the line-

absorption coefficient of the lines of H, $He\ I$ and $He\ II$ selected by PETRIE as the most sensitive indicators of spectral type in the O stars, these lines will not be studied here, but we will attempt to confirm the spectral type of our model by comparing the relative strengths of the combined doublet $\lambda\ 4267\cdot19$ of $C\ II$ and of $\lambda\ 4187\cdot05$ of $C\ III$, and of the pair of lines $\lambda\ 4819\cdot74$ of $Si\ III$ and $\lambda\ 4088\cdot86$ of $Si\ IV$. These lines have been selected either because they result from transitions between hydrogen-like levels and hence their f-values may be estimated (cf. below), or because an evaluation of the dipole moment matrix element necessary to compute the f-value is available.

The method of computing line profiles is straightforward, for the method of obtaining the emergent flux, outlined in the previous section, may be used. Since the lines to be studied arise from levels of high excitation, we shall consider the lines to be formed in absorption. Then the line-absorption coefficient per gram of star material is corrected for stimulated emission and treated as an addition to $\varkappa_\nu$. If F_c is the emergent flux in the continuous spectrum at wavelengths bordering the line, and if F_ν is the emergent flux at any frequency ν in the line, the residual intensity in the line is

$$R_\nu = F_\nu/F_c$$

and the absorption in the line is

$$A_\nu = 1 - R_\nu = \frac{F_c - F_\nu}{F_c}. \tag{57}$$

The line absorption coefficient per gram of star material corrected for stimulated emission is

$$l_\nu = \frac{\sqrt{\pi}\,e^2}{mc}\,\frac{fN^*}{\Delta\nu_D}\,H(a, v)\,(1 - e^{-h\nu/kT}), \tag{58}$$

where N^* is the number of atoms of the appropriate type per gram of star material excited to the lower level of the line, and

$$\Delta\nu_D = \frac{\nu_0}{c}\,\sqrt{\frac{2\,kT}{m_A}}.$$

Here m_A is the mass of the atom, k is Boltzman's constant, and ν_0 is the frequency of the centre of the line. The function $H(a,\nu)$ gives the shape of the line absorption coefficient broadened by collisional and radiation damping for atoms in thermal motion. This function has been tabulated by HJERTING (24) for a number of values of a and ν. Also recently a series expansion for $H(a,\nu)$ valid for small values of a has been given by HARRIS (25).

We have

$$H(a,\nu) = \frac{a}{\pi} \int_0^{\infty} \frac{e^{-y^2}}{(\nu-y)^2 + a^2} \, dy$$

where

$$\nu = \frac{\nu - \nu_0}{\Delta \nu_D}$$

and

$$a = \frac{\gamma}{4\pi \Delta \nu_D}.$$

The quantity γ is the damping constant for the line. For radiation damping

$$\gamma = \gamma_m + \gamma_n \tag{59a}$$

where γ_m is the width of the upper level and γ_n is the width of the lower level. It may be shown (cf. for instance, UNSÖLD (12), p. 172) that

$$\gamma_m = \sum_{n<m}' A_{nm} (1 - e^{-h\nu/kT})^{-1} + \sum_{n'>m}' A_{mn'} \frac{2 J_{n'}+1}{2 J_m+1} (e^{h\nu/kT}-1)^{-1}, \tag{59b}$$

where A_{nm} is the Einstein probability coefficient for spontaneous emission between two levels m and n which have total angular momentum quantum numbers J_m and J_n respectively.

The f-value occurring in equation (58) is the absorption f-value for the line in question. Its value for a line in a multiplet requires some consideration. According to CONDON and SHORTLEY (26) the absorption f-valve is given by

$$f(\alpha j, \alpha' j') = \frac{8\pi^2 m\nu}{3 e^2 h} \frac{S(\alpha j, \alpha' j')}{2j'+1}, \tag{60}$$

where α is the chief quantum number of the upper level, α' is the chief quantum number of the lower level, and j and j' are the total angular momentum quantum numbers of these levels respectively. The quantity $S(\alpha j, \alpha' j')$ is the theoretical strength of the line, a quantity which is symmetric in the upper and lower levels. For a line designated by

$$\alpha'^{2S+1} L'_{J'} - \alpha^{2S+1} L_J$$

of a multiplet which obeys L-S coupling, explicit forms may be found for the theoretical strength (cf. Condon and Shortley [26] p. 238). Using these expressions we can write

$$f(\alpha J, \alpha' J') = \frac{8\,\pi^2 m\nu}{3\,e^2 h} \left| (\alpha L \,|\, P \,|\, \alpha' L') \right|^2 \Psi(L, S, J, J'), \qquad (61)$$

where Ψ takes the following values depending in the type of transition.

type of transition	$\Delta L = 1$	$\Delta L = 0$
$J \to J+1$	$\dfrac{Q(J)\,Q(J+1)}{4\,(J+1)\,(2J+3)}$	$\dfrac{P(J+1)\,Q(J)}{4\,(J+1)\,(2J+3)}$
$J \to J$	$\dfrac{P(J)\,Q(J)}{4\,J\,(J+1)}$	$\dfrac{[R(J)]^2}{4\,J\,(J+1)}$
$J \to J-1$	$\dfrac{P(J)\,P(J-1)}{4\,J\,(2J-1)}$	$\dfrac{P(J)\,Q(J-1)}{4\,J\,(2J-1)}$

The table gives $\Psi(L, S, J, J')$.

Here

$$P(J) = (J - S + L)(J + S + L + 1)$$

$$Q(J) = (S + L - J)(J + S - L + 1)$$

$$R(J) = J(J+1) - S(S+1) + L(L+1),$$

and L is the largest of the two L-values occurring while J is the J-value belonging to that term. To obtain the f-value we need

now to evaluate $\left|(\alpha L \mid P \mid \alpha' L')\right|^2$. For a central field it may be shown (cf. CONDON and SHORTLEY [26], p. 132) that

$$\left|(\alpha L \mid P \mid \alpha' L-1)\right|^2 = \frac{e^2}{4L^2-1}\left(R_{\alpha L}^{\alpha' L-1}\right)^2, \tag{62}$$

where $\left(R_{\alpha L}^{\alpha' L-1}\right)^2$ is the square of the dipole matrix element of the radial part of the wave function. For central fields only transitions with $\Delta L = \pm 1$ are allowed. By combining equations (61) and (62) we find

$$f(\alpha L J, \alpha' L-1 J') = \frac{8\pi^2 m\nu}{3h}\left(R_{\alpha L}^{\alpha' L-1}\right)^2 \frac{\Psi(L,S,J,J')}{4L^2-1}. \tag{63}$$

It may be noted that

$$\left(R_{\alpha L}^{\alpha' L-1}\right)^2 = \left(R_{\alpha' L-1}^{\alpha L}\right)^2.$$

Consequently we may find the f-value for all transitions for which we know $\left(R_{\alpha L}^{\alpha' L-1}\right)^2$. If the energy levels concerned are hydrogen-like we can put

$$\left(R_{\alpha L}^{\alpha' L-1}\right)^2 = \left[R_{\alpha L}^{\alpha' L-1}(H)\right]^2 / Z^2 \tag{64}$$

where $\left[R_{\alpha L}^{\alpha' L-1}(H)\right]^2$ is the square of the radial matrix element for hydrogen, tabulated for instance by BETHE (27), and Z is the effective charge on the nucleus. Combining equations (61), (62) and (64) we find that the f-value for a line occurring between two hydrogen-like levels is

$$f(\alpha L J, \alpha' L-1 J') = \frac{8\pi^2 m\nu}{3h}\frac{\left[R_{\alpha L}^{\alpha' L-1}(H)\right]^2}{Z^2}\frac{\Psi(L,S,J,J')}{4L^2-1}. \tag{65}$$

Here L is the largest L-value occurring.

In a recent paper (28) BATES and DAMGAARD consider the calculation of the absolute strengths of spectral lines and show that the quantity $\left(R_{\alpha L}^{\alpha' L-1}\right)^2/(4L^2-1)$, which they call σ^2, may be evaluated approximately by neglecting the departure of the potential of an atom or an ion from its asymptotic Coulomb form. They show that this approximation is remarkably good for the

lighter elements, up to *Mg*, and for simple systems which are composed of one electron outside a closed shell, and that it yields useful information for complex systems which have unclosed shells. For many spectral lines of astrophysical interest this evaluation by BATES and DAMGAARD of $\left(R_{\alpha L}^{\alpha' L-1}\right)^2$ is superior to a hydrogenlike approximation.

It is of interest to find the sum of the *f*-values of all components of a multiplet arising from a given sub-level, characterised by J', of the lower term. To find this we evaluate

$$\sum_{J}' f(\alpha J, \alpha' J') = \frac{8\,\pi^2\,m\nu}{3\,e^2 h}\,\frac{1}{2\,J'+1}\sum_{J}' S(\alpha J, \alpha' J')$$

keeping J' fixed. Reference to CONDON and SHORTLEY (26) p. 238 enables us to evaluate the sum on the right side for the various types of multiplet that occur. In the case $\varDelta L = -1$

$$\sum_{J}' f(\alpha L J, \alpha' L-1 J') = \frac{8\,\pi^2\,m\nu}{3\,e^2 h}\left|(\alpha L\,|\,P\,|\,\alpha' L-1)\right|^2 L\,(2\,L+1). \quad (66)$$

In the case $\varDelta L = 0$

$$\sum_{J}' f(\alpha L J, \alpha' L J') = \frac{8\,\pi^2\,m\nu}{3\,e^2 h}\left|(\alpha L\,|\,P\,|\,\alpha' L)\right|^2 L\,(L+1), \quad (67)$$

and in the case $\varDelta L = +1$

$$\sum_{J}' f(\alpha L-1 J, \alpha' L J') = \frac{8\,\pi^2\,m\nu}{3\,e^2 h}\left|(\alpha L-1\,|\,P\,|\,\alpha' L)\right|^2 L\,(2\,L-1). \quad (68)$$

Since the lines we shall study belong to the case $\varDelta L = -1$ (see Table 12), we shall continue the discussion using only equation (66). Using equation (62) we find that.

$$\sum_{J}' f(\alpha L J, \alpha' L-1 J') = \frac{8\,\pi^2\,m\nu}{3\,h}\,\frac{L}{2\,L-1}\left(R_{\alpha L}^{\alpha' L-1}\right)^2. \quad (69)$$

When we compare this expression with the well-known formula for the oscillator strength in a one electron system (cf. for instance BETHE [27] p. 435),

$$f_{\alpha l - \alpha' l'} = \frac{1}{3} \frac{\max(l, l')}{2\,l' + 1} \left(\frac{\nu}{Ry} \right) \left(R_{\alpha l}^{\alpha' l'} \right)^2,\qquad (70)$$

where l' is the angular momentum quantum number of the lower state and (ν/Ry) is the frequency of the line in units of the Rydberg frequency, and when we put $l' = L - 1$, $l = L$ in equation (70), we find that

$$\sum_J f(\alpha\,LJ, \alpha'\,L - 1\,J') = f_{\alpha L - \alpha' L - 1}. \qquad (71)$$

Throughout this paragraph we are implicitly assuming that the frequency of all components of the multiplet arising from the sub-level J' is the same. If this is true then it is apparent that the f-value of any component may be found from the relation

$$\left.\begin{aligned} f(\alpha\,LJ, \alpha'\,L - 1\,J') &= \frac{f(\alpha\,LJ, \alpha'\,L - 1\,J)}{\sum_J f(\alpha\,LJ, \alpha'\,L - 1\,J)} \cdot f_{\alpha L - \alpha' L - 1} \\[2mm] &= \frac{\Psi(L, S, J, J')}{L\,(2\,L + 1)}\, f_{\alpha L - \alpha' L - 1}. \end{aligned}\right\} (72)$$

In his paper on τSco, Unsöld (29) effectively uses equation (72) to estimate the f-values of lines in multiplets. However, what he calls "f" is

$$f(\alpha\,LJ, \alpha'\,L'J') \cdot \frac{2\,J' + 1}{(2\,S + 1)(2\,L' + 1)}$$

for he combines with the f-value the factor $(2\,J' + 1)/(2\,S + 1) \cdot (2\,L' + 1)$ by which you must multiply

$$N_{r, s} = \frac{g_{r, s}}{u_r}\, e^{-\chi_{r, s}/kT} \qquad (73)$$

to get N^*, the number of atoms excited to the sub-level from which the line arises. Here, as usual, $g_{r, s} = (2\,S + 1)(2\,L' + 1)$, and $\chi_{r, s}$ is the excitation energy of the lower level of the line. Since there is no real advantage to working with the pseudo f-values introduced by Unsöld, and since this procedure may even lead to error if one should take these "f-values" and convert them into Einstein spontaneous emission probabilities by the relation

$$A(\alpha'J', \alpha J) = \frac{8\,\pi^2 e^2 \nu^2}{mc^3} \frac{(2\,J'+1)}{(2\,J+1)}\,f(\alpha J, \alpha'J'),$$

in order to compute the radiation damping constant of a line according to equations (59a) and (59b), it is preferable to compute the true f-values for the lines of L-S coupling multiplets by equations (63), (65), or (72).

In order to determine the radiation damping constant for the lines studied we shall compute the Einstein spontaneous transition probabilities by the relation

$$A(\alpha'J', \alpha J) = \frac{64\,\pi^4}{3\,h} \frac{\nu^3}{c^3}\,e^2 \left(R_{\alpha L}^{\alpha' L-1}\right)^2 \frac{\Psi(L, S, J, J')}{(4\,L^2-1)} \frac{(2\,J'+1)}{(2\,J+1)}. \quad (74)$$

We shall neglect collision damping. Of the lines chosen, only $Si\,IV\,\lambda\,4089$ is sufficiently strong that the exact value of the damping constant is of consequence. For this line RUDKJØBING (8) has shown that collision damping is not important.

The lines studied are given in Table 12 together with the relevant spectroscopic information. The necessary matrix elements, R^2, for obtaining the f-values and damping constants of the $C\,II$, $C\,III$ and $Si\,III$ lines were obtained by assuming these spectra to be hydrogen-like. The matrix-elements for $Si\,IV$ were found by the method of BATES and DAMGAARD (28). It is to be noted that according to equations (59) the radiation damping constant depends upon the temperature. For the $C\,II$, $C\,III$ and $Si\,III$ lines γ at $32,000°$ was used throughout the atmosphere, but for

Table 12.

Lines studied.

Spectrum	Designation	$j' - j$	λ	f	γ at $32,000°$
$C\,II$	$3d\,{}^2D—4f\,{}^2F°$	${}^3/_2—{}^5/_2$			
		${}^5/_2—{}^5/_2$	4267.19	1.11	1.69×10^{10}
		${}^5/_2—{}^7/_2$			
$C\,III$..........	$4\,{}^1F°—5\,{}^1G$	3—4	4187.05	1.44	2.22×10^9
$Si\,III$	$4f\,{}^3F°—5g\,{}^3G$	3—3			
		3—4	4819.74	1.25	3.97×10^9
$Si\,IV$	$4\,{}^2S—4\,{}^2P°$	${}^1/_2—{}^3/_2$	4088.86	0.751	4.02×10^9

the *Si IV* line γ was calculated at each depth in the atmosphere. In evaluating the damping constant account was taken of all possible transitions to the levels listed by Bacher and Goudsmit (30).

The line absorption coefficient per gram of star material corrected for stimulated emission was derived at each level in the atmosphere according to equation (58). The ionisation and excitation equilibria were computed at each level, and account was taken of the temperature dependence of the various partition functions involved. The function $H(a, v)$ was evaluated by the series expansion given by Harris (25). The monochromatic continuous absorption coefficient corrected for stimulated emission was also obtained at each level for the central frequency of each line, and then the relative absorption at several points in the line profile was computed by the method outlined above. The results obtained are given in Table 13. These points were plotted and the profile was integrated graphically to give the equivalent widths listed in Table 14. The relative amounts of C and Si to H used, are those found by Unsöld (29) for τSco, that is $N(H)/N(C) = 5\cdot8 \times 10^3$ and $N(H)/N(Si) = 1\cdot6 \times 10^4$.

Table 13.

Computed absorption line profiles*

$\Delta\lambda$	$C\,II\,\lambda\,4267\cdot19$	$C\,III\,\lambda\,4187\cdot05$	$Si\,III\,\lambda\,4819\cdot74$	$\Delta\lambda$	$Si\,IV\,\lambda\,4088\cdot86$
0.00 A	0.35	0.30	0.27	0.00 A	0.41
.07	.31	.26	.18	.10	.37
.14	.17	.14	.02	.20	.14
0.21	0.04	0.03	0.00	.40	.05
..	..	..	..	0.80	0.03

* The table gives absorption in the line in terms of the continuous spectrum at the wavelength in question.

The $C\,II$ "line", $\lambda\,4267\cdot19$, is a blended multiplet of three components. The two components arising from the sub-level with $j = 5/2$ have the same wavelength, hence we form a summed f-value for them as in equation (69). This summed f-value is the same as that for the one component arising from the level

with $j = 3/2$. We next assume that all components have the mean wavelength 4267·19 A, and find the desired line absorption coefficient by adding the contributions from each component. Since each component has the same damping constant, it follows that l_ν for the combined multiplet is given by formula (58) with f equal to the summed f-value for all components arising from either sub-level $j = 3/2$ or sub-level $j = 5/2$, and that N^* is the number of excited atoms given directly by the Boltzman equation (eq. [73]).

The $C\,III$ and $Si\,IV$ lines are single, consequently the procedure of forming l_ν is straightforward. The $Si\,III$ line is composed of two components which arise from the sub-level $j = 3$ of the lower term. Since these two components have the same wavelength we use a summed f-value, equation (69), and we note that in this case N^* is not given by Boltzman's equation directly; but by $N_{r,s} \times (2\,J'+1)/(2\,S+1)\,(2\,L'+1)$.

The strength of the lines in the model atmosphere may be compared with measurements made on high dispersion plates of the strengths of the same lines in $\tau\,Sco$, a $BO\,V$ star, by UNSÖLD (29), and in 10 Lac, an $O\,9\,V$ star, by ALLER (31).

The observed equivalent widths are given in Table 14 together with the computed equivalent widths. The observed and computed relative intensities $C\,II/C\,III$ and $Si\,III/Si\,IV$ are given in Table 15.

Table 14.

Equivalent widths*.

Line	Computed	$\tau\,Sco\,BO\,V$ (Unsöld)	10 Lac $O\,9\,V$ (Aller)
$C\,II\,\lambda\,4267$	0.099	0.115	0.081
$C\,III\,\lambda\,4187$	0.085	0.065	0.089
$Si\,III\,\lambda\,4820$......................	0.050	0.071	(<0.050)
$Si\,IV\,\lambda\,4089$	0.209	0.174	0.270

* in equivalent angstroms.

Since Aller does not measure the line $\lambda\,4820$ in 10 Lac, I estimate that its equivalent width is less than 0·050 E. A. It is not certain that the measurements by Unsöld and by Aller are

on the same scale, for the plates used, although of comparable dispersion, are not taken by the same telescope and spectrograph. This fact should not seriously affect the interpretation of the observed and computed relative intensities *C II/C III* and *Si III/ Si IV*, but it will prevent a precise determination of the abundance of carbon and silicon by matching the computed equivalent widths closely to the observed equivalent widths.

Table 15.

Relative intensities.

Ratio	Computed	τ Sco BO V (Unsöld)	10 Lac O 9 V (Aller)
C II/C III	1.17	1.77	0.91
Si III/Si IV	0.24	0.41	(< 0.18)

From the data of Table 15 we conclude that the spectral type of the model atmosphere is definitely earlier than *BO V* and somewhat later than *O 9 V*, say *O 9·5 V* on the scale of MORGAN, KEENAN and KELLMAN (23). R. M. PETRIE (4) classifies 10 Lac as an *O 8·5* star. On his scale the model atmosphere might just be an *O 9* star. The effective temperature of 36,800° which we have found for the model atmosphere is considerably higher than the excitation temperature of 30,700° found by Petrie for *O 9* stars from a study of the relative intensities of the *He II* and *He I* lines $\lambda 4542$ and $\lambda 4471$ respectively, and is also higher than the temperature based on the ionisation scale given by KUIPER (5).

The difference between effective temperature and excitation temperature found here for the *O 9* stars is in the same direction as that found for later type stars from curve of growth studies. This result occurs because of the rather great transparency of stellar atmospheres to radiation in the range $912 < \lambda < 1500 \text{A}$, which tends to increase the integrated emergent flux above that expected for the temperatures indicated by the opacity in the wavelength regions corresponding to the excitation of the commonly studied lines.

The dependence of the monochromatic optical depth, t_ν, on

Table 16.

The monochromatic optical depths, t_ν, at various wavelengths.

τ	$\lambda\,314$	$\lambda\,649$	$\lambda\,912\,\mathrm{v}$	$\lambda\,1006$	$\lambda\,1458$	$\lambda\,3646\,\mathrm{v}$	$\lambda\,4234$	$\lambda\,6251$
0.00	0.00	0.00	0.00	0.000	0.000	0.000	0.000	0.000
0.10	0.77	0.12	0.32	.013	.014	0.039	0.022	0.040
0.20	1.45	0.24	0.64	.023	.026	0.080	0.044	0.082
0.40	2.56	0.49	1.30	.041	.049	0.17	0.092	0.18
0.60	3.43	0.72	1.93	.059	.074	0.28	0.15	0.30
0.80	4.14	0.96	2.55	.078	.100	0.40	0.21	0.44
1.00	4.71	1.18	3.14	.097	.13	0.53	0.28	0.60
1.40	5.58	1.62	4.31	.139	.19	0.83	0.45	0.98
1.80	6.11	2.06	5.46	.186	.27	1.18	0.67	1.44
2.20	6.66	2.50	6.60	.236	.35	1.59	0.92	1.97
2.60	7.00	2.93	7.73	.289	.44	2.03	1.19	2.55
3.00	7.26	3.35	8.84	0.345	0.53	2.50	1.48	2.97

wavelength in the present model atmosphere is illustrated by the data of Table 16. The emergent monochromatic flux may be roughly evaluated by taking B_ν at the depth $t_\nu = 0 \cdot 60$. It is obvious from the data of Table 16 that the "temperature" of the emergent flux varies considerably with wavelength. In a line, the monochromatic optical depth varies rapidly with wavelength, as is illustrated by the data of Table 17, and it is a question what

Table 17.

t_ν in $\lambda\,4267$, $N(H)/N(C) = 5 \cdot 8 \times 10^3$.

τ	$\Delta\lambda = 0 \cdot 00\ \mathrm{A}$	$\Delta\lambda = 0 \cdot 07\ \mathrm{A}$	$\Delta\lambda = 0 \cdot 14\ \mathrm{A}$	$\Delta\lambda = 0 \cdot 21\ \mathrm{A}$
0.00	0.00	0.00	0.000	0.000
0.10	0.55	0.32	0.080	0.031
0.20	1.14	0.66	0.166	0.064
0.40	2.20	1.29	0.34	0.131
0.60	3.10	1.84	0.51	0.20
0.80	3.80	2.31	0.64	0.28
1.00	4.36	2.70	0.81	0.37
1.40	5.13	3.25	1.08	0.56
1.80	5.68	3.68	1.35	0.79
2.20	. .	4.08	1.65	1.05
2.60	. .	4.46	1.96	1.33
3.00	. .	4.82	2.28	1.64

optical depth, or temperature, should be taken as "characteristic" of the whole line, for the level at which $t_\nu = 0.60$ occurs differs greatly, depending on the distance from the line centre. The data of Table 17 illustrate nicely that the core of a line is formed in the outermost layers of the atmosphere, while the wings are formed at progressively deeper layers. In any case it is evident that whatever temperature is chosen in order that the actual process of line formation may be represented by line formation in a layer of gas at one temperature and pressure, this temperature will be less than the corresponding temperature for the continuous spectrum in the neighbourhood of the line, and that both of these temperatures will be less than the effective temperature, for the effective temperature is largely determined by the magnitude of the emergent flux in the region $912 < \lambda < 1500 \text{A}$, and in this region the "characteristic temperature" is high. Excitation or ionisation temperatures are effectively "characteristic temperatures" for the lines involved and hence bear a complicated relationship to the effective temperature of the atmosphere, which is defined by the integrated emergent flux.

The high effective temperature we have found for the $O\,9.5\,V$ stars, which is in accord with the estimate of RUDKJØBING (8) from his study of model atmospheres, means that the B stars are spread over a large range of effective temperature, for the effective temperature of $AO\ V$ stars seems to be close to $10,000°$ (32). The greatest spread in effective temperature probably occurs amongst the early B-type stars, for at the temperatures estimated to be characteristic of these atmospheres the peak of the black-body energy distribution curve moves into the range $912 < \lambda < 1500 \text{A}$. When this happens an excess of emergent radiation in this critical wavelength range will build up rapidly, and force up the effective temperature. It is difficult to estimate how high the effective temperatures of the absorption-line $O\,5$ or $O\,6$ stars may be. Consideration of the stability of atmospheres under the effects of radiation pressure (10), indicates that only stars of large surface gravity will have stable atmospheres at very high effective temperatures.

From Table 14 we see that the absolute strengths of the lines in the model atmosphere are intermediate between those observed in $\tau\,Sco$, $B0\ V$, and in 10 Lac, $O\,9\ V$. This result is in accord

with the spectral type of the model atmosphere being $O\,9{\cdot}5\,V$, and confirms the assumption that the relative abundances of C and Si to H used are representative of the chemical composition of early-type atmospheres. The actual abundances occurring cannot be far from the chosen abundances, for if the carbon abundance is reduced by a factor $0{\cdot}4$, the absolute strengths of the $C\,II$ and $C\,III$ lines are reduced to $0{\cdot}069$ E. A. and $0{\cdot}061$ E. A. respectively. These values are significantly lower than the observed line strengths. The ratio $C\,II/C\,III$ is nearly unchanged by this change in the carbon abundance, for it becomes $1{\cdot}13$ instead of 1.17. Since hydrogen is the dominant source of opacity in the wavelength range of the lines studied, departure of the real abundance of He from the assumed abundance of He will not affect the computed line strengths and the relative abundances of C and Si deduced therefrom by altering the contrast appreciably.

6. The limb-darkening of early type stars is difficult to establish from observations of eclipsing variables in which one or both components are O or B-type stars, and usually the observations are worked through with estimated values of the coefficient of limb-darkening. Since in the course of the computations for the net flux in the atmosphere we have obtained the monochromatic source function S_ν as a function of the optical depth, we can compute the emergent intensity as a function of the angle of emergence and can thus find the limb-darkening of the model atmosphere in various wavelengths. We have

$$I_\nu(0,\mu) = \mu^{-1} \int_0^\infty S_\nu(t_\nu)\, e^{-t_\nu/\mu}\, dt_\nu, \qquad (76)$$

where $I_\nu(0,\mu)$ is the monochromatic intensity emerging at the angle $\cos^{-1}\mu$ to the normal. Here t_ν is the monochromatic optical depth. The limb-darkening is expressed by

$$I_\nu(0,\mu)/I_\nu(0,1) = 1 - u + u\mu, \qquad (76)$$

where u is the coefficient of limb-darkening.

The values of $I_\nu(0,\mu)/I_\nu(0,1)$ given in Table 18 were found by integrating equation (75) numerically for values of μ equal to $1{\cdot}00$, $0{\cdot}50$, $0{\cdot}20$ and $0{\cdot}05$. At the limb, $\mu = 0{\cdot}00$, $I_\nu(0,\mu)$

Table 18.

The limb-darkening, $I_\nu(0, \mu)/I_\nu(0, 1)$, of the model atmosphere.

μ	$\lambda\,6251$	$\lambda\,4234$	$\lambda\,1006$	pure scattering
1.00	1.000	1.000	1.000	1.000
0.50	0.892	0.845	0.663	0.688
0.20	0.777	0.726	0.438	0.490
0.05	0.688	0.574	0.373	0.380
0.00	0.561	0.476	0.338	0.331

was put equal to $S_\nu(0\cdot0)$. Also given in Table 18 is the limb-darkening computed by CHANDRASEKHAR (33) for an atmosphere scattering according to the Rayleigh phase function, i. e. for electron scattering. The intensity $I_\nu(0,1)$ equals $1\cdot57 \times 10^{-3}$, $3\cdot17 \times 10^{-3}$ and $24\cdot69 \times 10^{-3}$ ergs/cm²/sec respectively at $\lambda\,6251$, $\lambda\,4234$ and $\lambda\,1006$. The wavelength $\lambda\,6251$ corresponds roughly to the effective wavelength of visual-red observations, while the wavelength $\lambda\,4234$ corresponds to the effective wavelength of photographic observations. At both these wavelengths hydrogen is the predominant source of opacity in the atmosphere. The limb-darkening was calculated at $\lambda\,1006$ also, because here electron scattering is the predominant source of opacity, and the
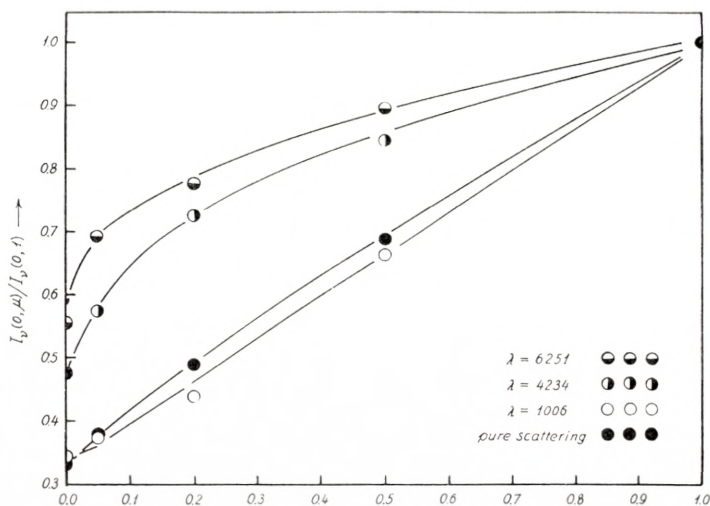

Fig. 2. The limb-darkening of the model atmosphere.

limb-darkening at $\lambda\,1006$ will be characteristic of electron scattering atmospheres.

The data of Table 18 are plotted in Figure 2 as a function of μ. The limb-darkening at $\lambda\,1006$ is closely that obtained by Chandrasekhar through exact computations of the limb-darkening expected in an atmosphere scattering according to Rayleigh's phase function. In the present computations the scattering was assumed to be isotropic. At $\lambda\,4234$ the electron scattering contributes a larger amount to the total opacity than at $\lambda\,6251$ and the limb-darkening curve is accordingly closer to the limiting curve for pure scattering.

An expression of the form of equation (76) was fitted to the plotted points by the method of least squares, yielding the following coefficients of limb-darkening: $u = 0\cdot35$ at $\lambda\,6251$, 0.44 at $\lambda\,4234$, $0\cdot65$ for pure scattering, and $0\cdot67$ at $\lambda\,1006$. From his study of the light curve of AO Cassiopeiae, FRANK BRADSHAW WOOD (34) concludes that the appropriate coefficient of limb-darkening for O stars is about $0\cdot6$. Since AO Cassiopeiae is a pair of O 8 supergiants we may expect electron scattering to be predominant even in the photographic and visual spectral regions. The value of the limb-darkening suggested by Wood is consistent with the results of the present computations which show that the limiting value of $u = 0\cdot65$ is approached when the opacity is predominantly due to electron scattering.

References.

(1) R. H. FOWLER and E. A. MILNE, M. N. **83**, 403, 1923 and **84**, 499, 1924.

(2) CECILIA H. PAYNE, *Stellar Atmospheres*, Harvard Monograph No. 1, 1925.

(3) A. PANNEKOEK, Ap. J. **84**, 481, 1936.

(4) R. M. PETRIE, Pub. Dom. Obs. Vol. 7, No. 21, 1947.

(5) G. P. KUIPER, Ap. J. **88**, 439, 1938.

(6) A. UNSÖLD, Zs. f. Ap. **21**, 1, 22, 229, 1942.

(7) B. STRÖMGREN, Pub. Cop. Obs. No. 127, 1940 and No. 138. The latter publication gives references to earlier work on model atmospheres by MILNE, McCREA, CHANDRASEKHAR, RUSSELL, UNSÖLD and PANNEKOEK.

(8) M. RUDKJØBING, Pub. Cop. Obs. No. 145, 1947.

(9) S. CHANDRASEKHAR, Ap. J. **101**, 328, 1945.

(10) A. B. UNDERHILL, M. N. in press.

(11) — Ap. J. **110**, 340, 1949.

(12) A. UNSÖLD, *Physik der Sternatmosphären* (Berlin: Julius Springer, 1938) p. 141.

(13) S. CHANDRASEKHAR, *An Introduction to the Study of Stellar Structure*, (The University of Chicago Press, Chicago, Illinois, 1939), p. 262.

(14) S. HUANG, Ap. J. **108**, 354, 1948.

(15) L. GOLDBERG, Ap. J. **90**, 414, 1939.

(16) B. STRÖMGREN, A. J. **53**, 107, 1947. The details of his method are unpublished yet.

(17) — A. J. **53**, 107, 1947; Ann. d'Ap. in press.

(18) A. UNSÖLD, Zs. f. Ap. **25**, 340, 1948.

(19) D. BARBIER and D. CHALONGE, Ann. d'Ap. **4**, 30, 1941.

(20) O. STRUVE and A. UNSÖLD, Ap. J. **91**, 365, 1940.

(21) D. R. INGLIS and E. TELLER, Ap. J. **90**, 439, 1939.

(22) G. R. MICZAIKA, Zs. f. Ap. **25**, 268, 1948.

(23) W. W. MORGAN, P. C. KEENAN, and E. KELLMAN, *An Atlas of Stellar Spectra*, (University of Chicago Press, Chicago, Illinois, 1943).

(24) F. HJERTING, Ap. J. **88**, 508, 1938.

(25) D. L. HARRIS III, Ap. J. **108**, 112, 1948.

(26) E. U. Condon and G. H. Shortley, *The Theory of Atomic Spectra*,
     (Cambridge University Press, 1935), p. 108.

(27) H. Bethe, Hb. d. Phys. **24,1**, 442, 1933.

(28) D. R. Bates and Agnete Damgaard, Trans. Roy. Soc. A, **242**, 101,
     1949.

(29) A. Unsöld, Zs. f. Ap. **21**, 22, 1941.

(30) R. F. Bacher and S. Goudsmit, *Atomic Energy States*, (McGraw-
     Hill Book Company Inc., New York and London, 1932).

(31) L. H. Aller, Ap. J. **104**, 347, 1946.

(32) A. B. Underhill, Ap. J. **108**, 83, 1948.

(33) S. Chandrasekhar, Ap. J. **105**, 435, 1947.

(34) F. B. Wood, Ap. J. **108**, 28, 1948.